TR 92063
ICAF 1867

(2)

DEFENCE RESEARCH AGENCY

Technical Report 92063

November 1992

The Growth of Short Fatigue Cracks in an Aluminium Alloy

by

R. Cook

Farnborough, Hampshire

DEFENCE RESEARCH AGENCY

Farnborough

Technical Report 92063

Received for printing 24 November 1992

THE GROWTH OF SHORT FATIGUE CRACKS IN AN ALUMINIUM ALLOY

by

R. Cook

SUMMARY

Fatigue tests have been carried out to establish the effects of various constant amplitude and standardised variable amplitude loading sequences on the growth of short and long cracks in 2024-T3 aluminium alloy. In most cases, the growth rates of short cracks were greater than those of long cracks for the same nominal stress intensity factor ranges, and short cracks grew at stress intensity factor ranges below the long crack threshold values. This Report describes and discusses the experimental crack growth results and compares them with predictions based on the FASTRAN crack closure model of Newman. The experimental work reported includes that which represented the United Kingdom contribution to the core programme of the AGARD cooperative programme on short crack growth behaviour.

Departmental Reference: Materials/Structures 363

LIST OF CONTENTS

1 INTRODUCTION

The use of Linear Elastic Fracture Mechanics (LEFM) in the damage tolerant design of aircraft structures is now widespread. Using this approach, it is assumed that flaws already exist at fatigue sensitive locations when the aircraft is built and that subsequent loading of the structure may cause these initial flaws to grow. The size of the assumed initial flaws must be small in order to demonstrate an acceptable fatigue endurance when the structure is subjected to the envisaged loading spectrum. Durability analyses are therefore required which will accurately predict the growth of cracks from these small initial flaws to failure. Inaccuracies in the analyses during the short crack growth period will have a large effect on the predicted fatigue endurance since a significant proportion of the total fatigue life is consumed within the short crack growth phase. Numerous investigations (*eg* Refs 1 to 6) have shown that the application of conventional LEFM to short cracks can result in an underestimation of fatigue crack growth rates. This approach leads to non-conservative life estimations and as a consequence much research has been focused in this area.

A specialists meeting[7] was arranged by the Structures and Materials Panel (SMP) of AGARD in 1982, at which conflicting evidence was presented as to the existence of this accelerated short crack growth behaviour. As a result of this meeting, an AGARD international cooperative working group was formed. Their tasks were; to develop a standard test method to measure short crack growth, to establish short crack growth data under a wide range of conditions, to develop models of short crack growth behaviour and to define the significance of the short crack effects. This Report describes some of the work carried out at the Defence Research Agency (formerly the Royal Aerospace Establishment) in support of this cooperative programme and some additional analytical work.

The AGARD short crack programme consisted of two parts, a core programme and a supplemental programme. The core programme[8] included the definition of standard test methods to be used, checking the accuracy of test loads and sequences at the different test sites and conducting fatigue tests on specimens made from a single batch of 2024-T3 aluminium alloy under a wide range of loading actions. The supplemental programme[9] consisted of a number of test programmes devised by individual participants to examine other test variables which were of particular interest to them. These variables included different materials and different loading actions to those used in the core programme and the application of short crack growth models to predict the observed behaviour. The DRA contribution to the supplemental programme[10] consisted of tests with the 2024-T3 material under different loading actions and some work on an aluminium-lithium alloy under various loading actions. This Report concerns the work carried out at the DRA using the common batch of 2024-T3 material. Further short crack growth work carried out using various aluminium-lithium alloys will be reported separately.

The term 'short crack' is imprecise and has different meanings to different people. A short crack to an engine-disc engineer may be micrometres in length, to an aircraft inspector it may be millimetres in length and to an offshore structures/ship engineer it may be centimetres in length. There has emerged from the literature over the past five years[11-13] some consensus on the form of short crack definitions. They are generally presented in the following form:

(a) Microstructurally short cracks – crack length is of the same order as the microstructural dimensions.

(b) Mechanically short cracks – crack length is of the same order as the plastic zone size.

(c) Physically short cracks – crack length is small compared to other dimensions of the body.

The definitions are clearly not mutually independent, nor are their effects on fatigue crack growth. For simplicity however, each category of short crack may be considered separately, as below.

Microstructurally short cracks cannot be assumed to be growing in a continuous medium. The rate of crack growth will vary as grain boundaries and inclusions are approached and subsequently passed. Crack arrest at grain boundaries may also occur if the applied stress is too low.

The growth of mechanically short cracks cannot be considered to be controlled by bulk remote stresses. In this case, crack tip yielding is large and consequently crack growth is determined by local elastic-plastic behaviour. Recent finite element analyses[14-16] have shown that short cracks can generate much larger plastic zones than long cracks when subjected to the same calculated stress intensity factor and that for small cracks subjected to relatively small stress intensity factors, these zones can be of the same order as the crack length. It is apparent that both of these types of crack violate the conditions assumed to exist in LEFM and it must be expected that the use of stress intensity factors to describe crack growth will not be accurate or appropriate.

Physically short cracks are perhaps better described as transitional cracks. They do not fall into the first two categories and are amenable to LEFM but they have not developed a sufficient plastic wake to be described as long cracks. Physically short cracks have lower closure levels than long cracks and therefore grow faster at the same calculated stress intensity factor.

It is apparent from these various definitions and observations that there may be a number of interactive causes of the anomalous behaviour of short cracks. The main aims of the present work are to determine the conditions under which short cracks propagate faster than long cracks subjected to the same calculated driving force, to measure the magnitude of

the effect and to assess its importance. In addition, the role of crack closure effects on mechanically and physically short cracks will be discussed in the light of experimental evidence, with particular reference to a crack closure based model.

2 TEST PROGRAMME

2.1 Objectives

The primary objective of the test programme was to produce crack propagation data at short and long crack lengths in order to establish the conditions under which rapid short crack growth occurred and the magnitude of the differences in growth rates between long and short cracks. It was necessary to test specimens under a wide range of loading actions and applied stress levels which were representative of those used to generate safe-life aircraft design data and those used to assess damage tolerance and durability requirements, such that a realistic appraisal of the impact of the short crack anomaly could be made. Typical loading conditions for various aircraft structures were therefore chosen; these are described in section 2.4.

In order to compare short and long crack growth rates it was necessary to calculate the stress intensity factor distributions. These calculations require the crack aspect ratio to be known as a function of crack length in the short crack specimens. This information was derived from data supplied by all of the participants in the AGARD short crack programme. Each participant was asked to perform one stop-off test for each crack propagation test condition undertaken. The stop-off test consisted of growing a crack/cracks in a specimen to within a predetermined range of crack lengths; three ranges were specified and allocated to different participants. Crack aspect ratios were measured by individual participants and a relationship between crack aspect ratio and crack length was derived.

2.2 Test specimens and materials

Crack growth data at short crack lengths were generated using side notch specimens as detailed in Fig 1. The semi-circular side notch was milled using final cuts of 0.25, 0.1, and 0.05 mm with a newly sharpened cutting tool, thus minimising residual stresses induced at the notch root. Chemical polishing of the notch area was also carried out to remove any machining marks and to deburr the edges of the specimen. This had an added advantage in that any shallow acting residual stresses, such as those induced by machining, would be eliminated by the removal of a thin layer of material. The chemical polish consisted of a 5 minute soak at 105°C in a solution of 80% (by volume) phosphoric acid, 5% nitric acid, 5% acetic acid and 10% water. The depth of material removed was approximately 0.02 mm All of the specimens were manufactured and supplied by United States Air Force Wright Patterson Aeronautical Laboratory.

End pads 2 mm thick were bonded to both sides and both ends of test specimens to avoid failures originating in the hydraulic wedge grips which were used during fatigue loading. An anti-buckling guide (see Fig 1) was lightly clamped to specimens which were to be subjected to compressive loading. PTFE shims were placed between the specimen and the anti-buckling guides to reduce the possibility of frictional load transfer through the guides.

Crack propagation data for long cracks was generated at NASA Langley using centre cracked panels as described in Ref 8. Additional long crack data were generated at DRA as detailed in section 2.4 using specimens of the type shown in Fig 2. These were manufactured from the same batch of material as that used to make the short crack specimens and the NASA Langley long crack specimens. The central notch was produced by spark erosion which gave a notch width of 0.58 mm, an end radius of 0.29 mm and a total length of 4.98 mm. An anti-buckling guide (see Fig 2) was used when compressive loads were applied.

The material used for all the specimens was to the specification 2024-T3. The original material was supplied in 2.3 mm thick sheets, 610 mm by 1830 mm and specimen blanks were cut such that the loading axis was in the rolling direction. The measured mechanical and chemical properties are given in Table 1. Typical grain dimensions were 95 μm in the rolling direction, 25 μm in the thickness direction and 55 μm in the specimen width direction. Inclusion particles were also observed and measured. They were approximately cylindrical in shape, the longitudinal axis being parallel to the rolling direction. Typical dimensions were 0.21 μm long with a diameter of 0.07 μm.

2.3 Test methods

All fatigue tests at DRA were conducted on an Instron 100 kN electro-hydraulic test machine. Alignment of the wedge grips was checked and specimens were shimmed to attain the specifications defined in Ref 8. The loading sequences were generated using an HP9836 computer. Achieved load levels were measured and errors corrected using an amplitude adaptive control loop[17] within the load generation programme. Short crack fatigue tests were stopped periodically and crack length measurements made using an acetate replica technique. The interval between measurements was chosen to give a minimum of 20 replicas per test on which cracks could be observed. A steady load was applied during replication equal to about 80% of the maximum load applied during the fatigue test, to open the fatigue crack and hence obtain a good replica impression. The replicas were examined under an optical microscope and the crack lengths measured. Cracks initiated in the side notch specimens at various locations but predominantly multiple cracks formed in the throat of the notch away from the specimen surfaces as shown schematically in Fig 3a. Cracks

were 'mapped' to aid crack identification when multiple cracking occurred. An example of a data chart showing such crack maps is shown in Fig 3b.

The procedure for generating long crack growth data was different from that described above for short crack data. Cracks of at least 2 mm in length were grown from either side of a central spark eroded slot at a relatively high stress level in a specimen of the type shown in Fig 2. The alternating load was then reduced by 6% and the cracks grown for a further 0.5 mm before the load was again shed by 6%. This load shedding procedure was continued until cracks failed to grow at a particular applied load range. This point was reached when no crack growth was observed after the application of one million cycles at one stress level under constant amplitude loading or after one load sequence for variable amplitude loading. The alternating load level was subsequently increased by 12% and the crack lengths monitored until failure occurred.

2.4 Test conditions

As discussed in section 2.1 the test conditions were chosen to represent a range of loading types and magnitudes which would typically be used in aircraft design and assessment. Table 2 summarises the load sequences used in the present work, including constant amplitude (R = -2, -1, 0 and 0.5), FALSTAFF and Gaussian sequences as selected for the AGARD core programme.

Constant amplitude testing was performed at stress ratios R of -2, -1, 0 and 0.5 at each of three different stress levels. Variable amplitude loading tests were carried out under the standard load sequences FALSTAFF, inverted FALSTAFF, Gaussian and Felix. All tests were carried out at a cyclic frequency of 15 Hz.

The FALSTAFF sequence represents a typical loading spectrum which might be experienced by the lower surface wing root of a fighter aircraft over a range of different mission types. The sequence was devised by a collaborative group[18] from measured load values on a range of service aircraft. It consists of 200 simulated flights containing a total of 35966 peak and trough load values. It contains gust, manoeuvre, landing and taxiing loads but is dominated by manoeuvre induced loads. Inverted FALSTAFF is a simple inversion of the FALSTAFF sequence, hence the manoeuvre and gust loads are predominantly compressive and the landing and taxi loads are predominantly tensile. It is representative of a sequence of loads which may be experienced by an upper surface wing root.

The standard Gaussian sequence was also defined by a collaborative group[19] as a general purpose fatigue testing sequence. It is a narrow bandwidth sequence and is representative of the loading response of a single degree of freedom structure subjected to random load inputs. The sequence is so named as the frequency of occurrence distribution of load level crossings is approximately that of a stationary Gaussian process. It consists of about one million cycles, the peak and trough values of which are defined by 32 discrete

values. The mean level of each transition is close to zero load and hence the overall sequence has a stress ratio value R approximately equal to -1.

The Felix sequence was defined by a collaborative group[20] from measurements on various helicopters with semi-rigid rotors. It represents a typical loading sequence which might be experienced by the lower blade root of a semi-rigid rotor over a wide range of mission types. It consists of 140 simulated flights and contains about 4.5 million peak and trough load values.

3 FATIGUE TEST RESULTS

Crack lengths were measured and crack maps produced for all short crack test sequences as described in section 2.3. Multiple cracking occurred in many tests and frequently these cracks coalesced. Cracks growing on parallel paths some distance apart did not necessarily coalesce but some interaction in terms of shielding may have taken place. Similarly when cracks approached each other before coalescence, some interaction would be expected and they could not be considered as independent cracks. It was necessary to derive some rules which defined when cracks could be considered to be growing independently. The following rules were made[8] and are referred to as the 'non interaction criteria'.

(a) Where cracks are in line with each other and when the distance between the adjacent crack tips is less than the length of the longest crack, then subsequent data from both cracks must be rejected. In this case it is expected that as the crack tips approach each other the rate of growth of each would be accelerated.

(b) Where cracks intersect the same line parallel to the loading axis of the specimen and when the distance between the two cracks is less than the length of the larger then subsequent data from the smaller is rejected. In this case the larger crack would be expected to relieve stresses in the region of the shorter crack and hence the shorter crack would grow more slowly.

(c) After two cracks have joined, crack growth rate data are rejected from both cracks until the combined crack length is twice that of the combined crack length at the time of coalescence. This is to allow for the development of a full crack front for the combined crack.

Up to five cracks were classified as the main cracks in each specimen. Data were recorded for each of the main cracks only where the non-interaction criteria were met. Crack growth rates were determined from the length/cycles data by calculating the linear slope between consecutive data pairs (secant method). Stress intensity factors were calculated using the full applied stress range from the approximate solution of Newman[21]

which requires a knowledge of the crack aspect ratio. The following aspect ratio – crack length relationship was derived from data obtained from experiments described in section 2.1.

$$c/a = 0.9 - 0.25(a/t)^2 \quad (1)$$

where c = crack depth,

a = ½ crack length for bore cracks,

= crack length for corner cracks

and t = specimen thickness.

Figs 4 to 7 show the constant amplitude short crack propagation data obtained for the stress ratios R = 0.5, 0, -1, and -2 respectively. Also shown in these figures as solid lines are the equivalent long crack data derived by Philips[8]. Variable amplitude short crack propagation data are presented in Figs 8 to 11 for the cases of FALSTAFF, inverted FALSTAFF, Gaussian and Felix respectively. Also shown in Figs 8, 10 and 11 are solid lines representing the equivalent long crack data derived by Phillips (FALSTAFF), Heuler (Gaussian) and Cook (Felix). The full experimental data sets, including data from all participants in the AGARD short crack core programme, are plotted in Figs 4 to 11 to give a more statistically significant basis on which comparisons can be made. Trends in the experimental data are evident in the complete database which cannot be easily observed from the DRA database alone.

4 MODELLING OF CRACK GROWTH

The FASTRAN model of Newman[22] was used to predict short crack growth behaviour. It is based on the Dugdale model but is modified to leave plastically deformed material in the wake of a growing crack. The model requires inputs relating to material properties, loading conditions and specimen geometry. The average measured mechanical properties of the material are given in Table 1. Other material properties required in the model included a description of crack growth rates as a function of effective stress intensity factors. Long crack propagation information was derived from the work of Hudson[23] for fast crack growth rates and from Phillips[24], for slower crack rates. The effective stress intensity factor range was determined by calculating crack opening stresses using the method of Newman[25]. Approximately plane strain conditions were assumed to exist from the start of each test until slant crack growth was first observed, and approximately plane stress conditions were assumed to exist when the transition from flat to slant crack growth was complete. The theoretical constraint factors for these two situations are $\alpha = 3$ for plane

strain and $\alpha = 1$ for plane stress. However, values of 1.73 and 1.1 were chosen to best fit the closure measurements made in the long crack tests of Hudson and Philips. In view of the uncertainty of the effect of thickness on stress state with such thin specimens, the use of α as a 'fitting parameter' was considered acceptable. In the transition phase from flat to slant crack growth, the constraint factor α was varied linearly with log crack rate. Thus α was defined entirely in terms of crack rate.

The same restraint conditions were assumed to apply in the short crack growth specimens and the constraint factor α was determined in the application of the FASTRAN model solely from crack growth rate calculations. Surface crack lengths were determined as a function of applied load cycles using the FASTRAN programme for all of the test conditions described in section 2.4 with the exception of the Felix sequence, where modification to the FASTRAN model would have been required. The results using the FASTRAN model are compared on a crack rate versus applied stress intensity factor basis with those measured experimentally. Crack rates were determined in both cases using the secant method described in section 3. Stress intensity factors were calculated using the same procedure for the experimental and predicted data as described in section 3. The experimental and predicted crack growth rates are presented in Figs 12 to 18. Experimental results are shown as individual points and predictions are shown as solid curves.

Crack opening stresses were also calculated using the FASTRAN program for the various loading conditions. Calculated values for the constant amplitude loading cases are shown in Fig 19 as a function of crack length (across the throat of the notch). For clarity, results are shown at only one of the three stress levels for each stress ratio R (predictions at all three stress levels are very similar at each R ratio). Calculated crack opening stresses are shown in Fig 20 for FALSTAFF and inverted FALSTAFF at each of the three test stress levels. Fig 21 shows the predicted opening stress levels for Gaussian loading.

5 DISCUSSION

5.1 Constant amplitude test results

Short crack propagation data are presented in Figs 4 to 7 for the stress ratios of R = 0.5, 0, -1 and -2 respectively. Also shown on these figures as solid lines are measured long crack propagation data. It can be seen from Fig 4 that for R = 0.5 loading, the short crack data do not exhibit a clear threshold value as observed in the long crack propagation data and short cracks are observed to grow at ΔK values below the long crack threshold value. This is due mainly to the different types of test which were used to generate the crack propagation data. Long crack data were generated by a load shedding procedure and in the threshold region cracks were relatively long (tens of millimetres) and had a well developed plastic wake. The effective stress intensity factor range, ΔK, in this

region was therefore likely to be slightly lower than the applied ΔK due to crack closure induced by a combination of surface roughness, plastic wake and possibly crack surface corrosion. The difference between effective and applied ΔK for long cracks will be referred to throughout this Report as long crack closure. Conversely, short crack data were generated from freely initiated cracks in a side notched specimen (see section 2.2) and data obtained in the low ΔK/threshold region were thus obtained from very short cracks which had just initiated and were effectively closure-free. The effective ΔK for short cracks was therefore greater than the effective ΔK for long cracks and hence short cracks grew at applied ΔK values below the long crack threshold. A short crack threshold is likely to exist but will be controlled by crack arrest at grain boundaries or inclusions. Further work is required to define short crack threshold conditions. At higher ΔK values, short crack growth rates at R = 0.5 were slower than those for long cracks, probably due to the notch root plasticity induced by the high applied stress levels in the short crack tests, causing crack retardation.

Crack growth rates under R = 0 loading (see Fig 5), show better agreement between long and short cracks at ΔK values above the long crack threshold than was observed under R = 0.5 loading. This is to be expected as the maximum applied stress levels in the short crack tests under R = 0 loading are much lower than those used in the R = 0.5 tests and notch root plasticity only occurs at the highest stress level. Thus the notch root plasticity which caused crack retardation in the short crack R = 0.5 tests is absent in the R = 0 tests, hence short and long crack growth rates become coincident when short cracks grow beyond the physically short regime. Short crack data under R = 0 loading at ΔK values below the long crack threshold however show a greater divergence from the long crack growth data than under R = 0.5 loading and also exhibit a stress level dependence. The reason for the greater divergence can again be explained in terms of long crack closure. The effective ΔK for long cracks is lower than the applied ΔK as already explained and under R = 0 loading the difference between these values will be greater than under R = 0.5 loading as cracks will be closed over a greater part of the loading cycle. Short cracks however will be effectively closure free at low ΔK values at both stress ratios and therefore the short crack effective ΔK will be approximately equal to the applied ΔK. Differences between long and short crack crack growth data at low ΔK values will therefore be more marked at R = 0 than at R = 0.5. This argument can be extended to other R values *ie* as the R ratio is decreased a greater divergence between long and short crack growth data is expected at low ΔK values as a greater divergence between effective ΔK and applied ΔK occurs.

The stress level dependence of short crack growth rates below the long crack threshold can be seen in Fig 5, where for any particular ΔK value cracks subjected to higher stress levels propagate at a faster rate than those at lower stress levels. This means that for a particular ΔK value shorter cracks (higher stresses) grow faster than longer cracks (lower

stresses). This can be explained by considering the closure levels of short cracks. The measurement of short crack closure levels is extremely difficult and so a qualitative explanation of the stress level dependence is given based on closure levels predicted by the FASTRAN model. Fig 19 shows the predicted closure levels of short cracks under constant amplitude loading at a range of stress ratios. At very short crack lengths where the local stress level is extremely high, large crack tip plastic zones form which effectively hold the crack open. Under R = 0.5 loading, short cracks are fully open throughout the applied loading cycle but at stress ratios of less than or equal to zero, closure levels are seen to be a function of crack length. Closure levels increase with an increase in crack length (Fig 19), hence shorter cracks will be subjected to a larger effective ΔK than longer cracks and propagate more quickly. This will be referred to throughout this Report as short crack closure. It is expected therefore that stress level dependence will be present in short crack tests where the stress ratio is equal to or less than zero and will become progressively more marked as the stress ratio decreases. Thus, the stress level dependence shown in Figs 5 to 7 may be explained by considering a specific value of ΔK (say 2 MPa . $m^{1/2}$) where data points shown for the high stress levels will involve shorter cracks and lower closure levels than in the case of corresponding data points obtained for the lower stress levels.

The assumption of closure free short cracks made earlier infers that closure will occur at zero or compressive loads for low ΔK values under negative stress ratio conditions. It can be seen from Fig 19 that the FASTRAN model predicts that effective ΔK values for short cracks approach applied ΔK values as the crack length tends to zero and that differences between short and long crack closure levels increase as stress ratio decreases. The predicted closure levels for R = -1 and -2 are a function of crack tip plasticity; notch root plasticity only occurs at the highest applied stress level under R = -2 loading. Crack growth data at stress ratios of R = -1 and R = -2 are presented in Figs 6 and 7 respectively. It can be seen that short crack data deviate from long crack data more markedly as the stress ratio decreases and the stress level dependence also increases as the stress ratio decreases. This was qualitatively explained in the foregoing discussion in terms of long and short crack closure.

The effect of compressive notch root plasticity was demonstrated by constant amplitude tests conducted under entirely compressive loading. Two test stress levels were used, giving gross section compressive stresses of 120 and 150 MPa, but cracks only grew under the higher applied stress level of 150 MPa. Very limited crack growth data were obtained from these tests and are not presented here but the fact that cracks grew shows that tensile residual stresses, induced by notch plasticity, resulted in an effective ΔK greater than the short crack threshold. The applied compressive stress level of 120 MPa only caused marginal plasticity ($K_t \cdot S_{max}/\sigma_{ys} = 1.07$) which would not be expected to result in significant tensile residual stresses. At the stress level of 150 MPa, however, significant

plasticity occurred ($K_t \cdot S_{max}/\sigma_{ys} = 1.33$), and the associated tensile residual stresses would be expected to result in some crack growth. Compressive notch plasticity is also of importance when considering variable amplitude loading sequences which contain high compressive loads, such as inverted FALSTAFF, which are discussed in the next section.

5.2 Variable amplitude test results

Crack propagation data for short and long cracks obtained under FALSTAFF loading are presented in Fig 8. It can be seen that short cracks generally propagate faster than long cracks at equivalent ΔK values. There also appears to be a slight dependence of short crack growth rate on applied stress level, again showing that shorter cracks (higher stresses) propagate faster than longer cracks (lower stresses) at equivalent applied ΔK levels. An examination of the predicted crack opening levels (see Fig 20) shows a clear dependence of closure level on crack length up to about 0.2 mm, thereafter the dependence is less marked but a gradual increase in closure level with increasing crack length is observed. This would qualitatively explain the stress level dependence at short crack lengths where the effective ΔK reduces as crack length increases giving rise to short cracks (high stresses) growing faster than long cracks (low stresses) at equivalent applied ΔK values. However the situation is complicated by the high tensile loads in the FALSTAFF sequence which cause different degrees of notch root plasticity and residual compressive stresses at different applied stress levels. Notch root plasticity has the effect of reducing crack growth rates in short crack tests; the greatest reduction being associated with the highest applied stress level.

Crack propagation data for short cracks obtained under inverted FALSTAFF loading are presented in Fig 9. Stress level dependence of short cracks is again observed which is caused by a combination of two parameters, crack tip plasticity which depresses closure levels and notch root plasticity in compression which results in tensile residual stresses; both are a function of crack length. Residual stresses due to notch plasticity induced during FALSTAFF and inverted FALSTAFF loading, should be approximately equal but of opposite sign. Crack tip plasticity however will be greater under FALSTAFF loading due to the higher tensile loads in the sequence. Crack growth rates under FALSTAFF loading are controlled by a combination of two opposing effects; extensive crack tip plasticity which reduces the closure level and notch plasticity which results in a compressive mean stress effectively increasing the closure level. In contrast, under inverted FALSTAFF loading crack growth rates are controlled by two additive effects; notch plasticity which creates tensile residual stresses, effectively depressing the closure level and limited crack tip plasticity which further depresses the closure level. In view of the small effect of crack tip plasticity on crack growth predicted for inverted FALSTAFF loading, it is concluded that the high crack growth rates observed are primarily due to notch plasticity.

The growth rates of short cracks under FALSTAFF and inverted FALSTAFF loading are compared in Figs 22 to 24 for the cases of 275, 205 and 170 MPa peak tensile and compressive stresses respectively. It can be seen that the growth rates under both sequences are similar at all three stress levels. It should be remembered that the ΔK values plotted in these figures are based on the full stress range from the maximum to the minimum applied loads and are thus equal for both sequences at each stress level. It can be concluded that the alternating stress experienced by the crack tips must have been similar under both sequences. The observations are supported by the predicted closure levels shown in Fig 20, where the dotted line in each loading case represents the maximum stress level applied in the sequence and the solid curve represents the crack closure stress. It is evident that the closure levels under inverted FALSTAFF loading give rise to similar crack tip stress ranges (distance between the dotted and solid curves) to those in the equivalent FALSTAFF tests.

Crack propagation data for short and long cracks obtained under Gaussian loading are presented in Fig 10. Unfortunately, the long crack data does not cover a low enough range of ΔK values to allow a direct comparison with the short crack data. However, it can be seen that even at high ΔK values where reasonable agreement between long and short crack growth data is expected, a significant discrepancy between them exists. Once again short cracks propagate faster than long cracks at the same applied ΔK values. The differences in growth rates between short and long cracks is much more marked than under FALSTAFF loading despite the similar applied stress ranges. This is because of the differences in sequence stress ratios and relative bandwidths. The high stresses in the FALSTAFF sequence are all applied in tension at positive stress ratios and being a broad band sequence, are not followed by large compressive stresses. These higher tensile loads result in a compressive residual stress zone due to notch plasticity which retards crack growth. The stress ratio of the Gaussian sequence is approximately equal to -1 and has a narrow bandwidth such that any high tensile loads are followed immediately by compressive loads of approximately equal magnitude. This causes reversed plasticity which results in a residual stress free zone around the notch, *ie* the retardation of short cracks due to notch plasticity observed under FALSTAFF loading does not occur under Gaussian loading. Both sequences however create crack tip plasticity due to high loads which depress crack closure levels and hence accelerate short crack growth. The result under Gaussian loading is a large difference in growth rates between short and long cracks caused by crack tip plasticity alone. As observed earlier, under FALSTAFF loading the two plasticity effects act in opposition and result in a much smaller difference between short and long crack growth rates. A slight stress level dependence can be seen in Fig 10 under Gaussian loading which is accounted for by the closure level dependence on crack length, as shown in Fig 21.

Propagation rates of short and long cracks under Felix loading are presented in Fig 11. The Felix sequence is similar to the FALSTAFF sequence in terms of maximum and minimum stress levels applied. The plastic zones associated with the notch and the crack tip will therefore be of a similar size under both test sequences. Since short crack growth rates are essentially determined by these two parameters, it may be expected that similar crack growth behaviour will also occur. It can be seen from a comparison of Figs 8 and 11 that short crack growth rates are indeed similar under both loading sequences. The long crack growth behaviour under Felix loading is however different to that under FALSTAFF loading. The result is that under Felix loading whilst short cracks grow at ΔK values below the long crack threshold, short cracks appear to propagate more slowly than long cracks at ΔK values above the long crack threshold. This requires further investigation but may be a function of sequence length. The relatively long Felix sequence (2.2×10^6 cycles) is not applied in its entirety in the short crack tests and is applied twice in the long crack tests. The load spectra in the long and short crack test are not therefore entirely comparable.

5.3 Crack growth rate predictions

Crack growth rate predictions are presented, along with the experimental data described earlier, in Figs 12 to 18 for each of the loading conditions. The FASTRAN model qualitatively predicts the trends observed in the experimental data *ie* the dependence of short crack growth rate on stress level, stress ratio and crack length. Quantitative agreement is also very good in most cases, although predictions at ΔK values above the long crack threshold are generally less accurate than at lower ΔK values. This is particularly noticeable at the stress ratio of 0.5 shown in Fig 12, and is probably due to the stress state assumptions made in the predictive model. The high stress levels used in the $R = 0.5$ tests will have caused extensive notch root plasticity which, due to the small specimen thickness, would effectively create plane stress conditions. In the model however, it is assumed that plane strain conditions exist until a crack growth rate of 9×10^{-5} mm/cycle is reached and that plane stress conditions are only achieved when the crack growth rate exceeds 7.5×10^{-4} mm/cycle. Accordingly the notch root plastic zone sizes calculated in the model are based on plane strain rather than plane stress assumptions and will hence be smaller than expected. This will cause the predicted crack growth rates to be higher than expected at crack lengths greater than the calculated plane strain plastic zone size until a growth rate of 7.5×10^{-4} mm/cycle is achieved. In the case of $R = 0.5$ loading predictions, the plane strain notch root plastic zone size is zero at the lowest stress level and extremely small at the other two stress levels and growth rates of 7.5×10^{-4} mm/cycle are never attained. It is expected therefore that predictions will be too high over the entire range of experimental measurements. This is an oversimplification of the expected errors as in practice cracks may grow under plane stress conditions within the influence of the notch root plastic zone and

then revert to plane strain conditions for some distance before returning once more to plane stress. This will affect both the rate of crack growth and the shape of the crack growth curve. A similar effect is expected in all tests where high stress levels are applied and significant notch root yielding occurs. Such conditions occur under R = 0.5, FALSTAFF and Felix loading conditions. An examination of Figs 12 and 16 for R = 0.5 and FALSTAFF loading respectively show this tendency to over predict the short crack growth rates. Predictions under Felix loading were not carried out as this option was not available in the FASTRAN program.

Crack growth rate predictions under R = 0.5 loading at a stress level of 195 MPa (see Fig 12), show no crack growth. The stress level has to be increased to over 200 MPa before any crack growth is predicted. This is in reasonable agreement with the experimental data where a number of specimens remained unbroken after testing at 195 MPa. This was also the case for predictions made at the lowest stress level (170 MPa) under inverted FALSTAFF loading conditions. It can be seen from Fig 17 that the predicted growth rates are much lower than those measured at the two higher stress levels and that at 205 MPa the predicted crack rate reduces markedly at about 20 MPa . $m^{1/2}$.The increasing closure level (Fig 20) reduces the effective ΔK and hence crack growth becomes discontinuous as progressively fewer cycles create ΔK values above threshold and eventually the growth rate decreases rapidly. Predictions at the lowest stress level showed little crack growth and this was in a highly discontinuous form.

5.4 Alternative crack growth models

Detailed explanation of the fatigue test results have been presented in terms of crack closure levels only. Other investigators have explained their test results in terms of crack growth interaction with grain boundaries and inclusions: when cracks are microstructurally short it is argued that their growth is dominated by their ability to grow past barriers such as grain boundaries. As a short crack approaches a grain boundary its growth rate will reduce and may even arrest. Further growth of the crack after arrest, or an increase in growth rate of a slowed crack, will occur when sufficient plasticity has developed in the adjacent grain. The picture is therefore of cracks continuously slowing down as they approach barriers and speeding up as they grow past them. Measurements of cracks in experimental programmes are generally made at intervals which are too infrequent to observe this detailed behaviour. A more detailed experimental study would be required to verify this postulated behaviour .

Undoubtedly the growth of short cracks in 2024-T3 alloy will be governed by both barrier interactions and variations in crack closure level. Modelling of the barrier interactions clearly requires statistical knowledge of size and distribution of microstructural features and quantification of their effects on crack growth rate. Models will therefore be probabilistic and upper and lower bound curves of growth rates could be defined based on

the closest and furthest likely spacing of barriers. It is planned that such modelling will be attempted and compared with the test results and with FASTRAN predictions. The need for a hybrid model involving the two approaches will be considered.

5.5 Impact of short crack growth data on damage tolerant design

The impact of the present work on the damage tolerant design of aircraft structures is complex. Clearly the sizes of the cracks which deviated from conventional long crack growth behaviour, are too short to be reliably detected by current NDI methods. This is true for global inspections of complete aircraft structures but may not be the case for specific locations such as strip down inspection of engine components. In terms of structural integrity of airframes, where cracks are monitored by NDI, short crack growth behaviour will not be a consideration. The safety of structures which contain MSD at fastener holes (principally fuselage) has been of particular concern in the last few years. The assumption that cracks will not initiate and grow in such areas may be in error because small cracks may be initiated by corrosion and then grow at very small ΔK values below the long crack threshold. In these circumstances the safety of the structure could be at risk if detailed inspections are not instigated.

In terms of durability, accelerated short crack growth could have a significant effect. The impact on durability is clearly demonstrated by the test results and may be important depending on the type and magnitude of loading experienced by the component and the precise damage location. Stress concentrations subjected to compression dominated loading, for example upper wing structure, are clearly an area of particular concern. This was demonstrated by the test results under inverted FALSTAFF loading, where accelerated short crack growth was particularly evident. Similar but less marked short crack effects were also found in tests where high tensile loads were applied. The acceleration effects would have been more marked but for the retarding compressive residual stresses caused by notch root yielding. Thus a case where short cracks initiate and grow from material or manufacturing defects under high tensile loads, and which are not influenced by geometric stress concentrations, is of concern as accelerated short crack growth is likely to be severe. This situation may occur in any highly loaded structural area and is therefore of considerable importance in durability assessment.

6 CONCLUSIONS

Fatigue testing has been carried out to establish the effect of various constant and variable amplitude loading sequences on the growth of short and long cracks in 2024-T3 alloy, and the results have been compared with predictions based on a crack closure model. The main conclusions of this study are:

(1) Under constant amplitude loading at stress ratios $R \leq 0$, short cracks grew faster than long cracks when subjected to the same applied alternating stress intensity factors. Additionally short crack growth rates were dependent on the applied stress level; this dependence became more marked as the stress ratio decreased.

(2) Under all of the constant and variable amplitude loading sequences used, short cracks grew at alternating stress intensity factor ranges which were less than the corresponding long crack threshold values.

(3) Under FALSTAFF, inverted FALSTAFF, Felix and Gaussian loading sequences, short cracks grew faster than long cracks subjected to the same applied stress intensity factor ranges.

(4) Short crack growth rates were similar under FALSTAFF and inverted FALSTAFF loading at equivalent stress ranges.

(5) The observed short crack growth behaviour may be explained in terms of the combined effects of notch root plasticity and crack tip plasticity on crack closure stress levels.

(6) In most cases, and in particular where notch root plasticity was insignificant, fatigue crack growth rates predicted by the FASTRAN crack closure model were in good agreement with experimental observations.

Table 1

MECHANICAL AND CHEMICAL PROPERTIES OF 2024-T3 ALUMINIUM ALLOY SHEET

Average measured mechanical properties of 2024-T3

Ultimate tensile strength MPa	0.2% proof stress MPa	Modulus of elasticity MPa	Elongation (51 mm gauge length) %
495	355	72000	21

Nominal chemical composition of 2024-T3 aluminium alloy sheet

	%
Silicon	0.16
Iron	0.33
Copper	4.61
Manganese	0.57
Magnesium	1.51
Chromium	0.02
Zinc	0.06

Aluminium balance

Table 2
FATIGUE TEST PROGRAMME

Loading	Maximum gross stress (MPa) S_{max}	$\frac{K_T S_{max}}{\sigma_{ys}}$	$\frac{K_T S_{min}}{\sigma_{ys}}$
Constant	75	0.67	-1.34
Amplitude	60	0.54	-1.07
R = -2	50	0.45	-0.89
Constant	105	0.94	-0.94
Amplitude	80	0.71	-0.71
R = -1	70	0.63	-0.63
Constant	145	1.29	0
Amplitude	120	1.07	0
R = 0	110	0.98	0
Constant	225	2.00	1.00
Amplitude	205	1.82	0.91
R = 0.5	195	1.74	0.87
Constant	0 (-150 min)	0	-1.34
Amplitude	0 (-120 min)	0	-1.07
R = ∞			
FALSTAFF	275	2.45	-0.66
	205	1.82	-0.49
	170	1.52	-0.40
Inverted	74.04 (-275 min)	0.66	-2.45
FALSTAFF	55.19 (-205 min)	0.49	-1.82
	44.74 (-170 min)	0.40	-1.52
Gaussian	170	1.52	-1.52
	145	1.29	-1.29
	125	1.12	-1.12
Felix	200	1.80	-0.50
	185	1.66	-0.46
	170	1.52	-0.43

REFERENCES

No.	Author	Title, etc
1	S. Pearson	Initiation of fatigue cracks in commercial aluminium alloys and the subsequent propagation of very short cracks. *Eng. Fract. Mechanics* **7**, No. 2 pp 235-247 (1975)
2	D. Taylor J.F. Knott	Fatigue crack propagation behaviour of short cracks; the effect of microstructure. *Fat. Eng. Mat. & Struct.* **4**, No. 2 pp 147-155 (1981)
3	M.H. El Haddad N.E. Dowling T.H. Topper K.N. Smith	J integral applications for short fatigue cracks at notches. *Int. J. of Fract.* **16,** No. 1 pp 15-30 (1980)
4	R. Cook P.R. Edwards R.F.W. Anstee	*Crack propagation at short crack lengths under variable amplitude loading.* RAE Technical Report 82038 (1982)
5	J. Lankford	The growth of small fatigue cracks in 7075-T6 aluminium. *Fat. Eng. Mat. & Struct.* **5**, No. 3 pp 233-248 (1982)
6	Y. Furuya H. Shimada	Propagation of 'small fatigue crack' initiated from notch-root. *Eng. Fract. Mechanics* **19,** No. 1 pp 41-48 (1984)
7		*Behaviour of short cracks in airframe components.* AGARD Conference proceedings AGARD-CP-328 (1982)
8	J.C. Newman Jr. P.R. Edwards	*Short-crack growth behaviour in an aluminium alloy – an AGARD cooperative test programme.* AGARD Report AGARD-R-732 (1988)
9	P.R. Edwards J.C. Newman Jr.	*Short-crack growth behaviour in various aircraft materials.* AGARD Report AGARD-R-767 (1990)
10	R. Cook	*The growth of short fatigue cracks in 2024 and 2090 aluminium alloys under variable amplitude loading.* *Short-crack growth behaviour in various aircraft materials.* AGARD Report AGARD-R-767 (1990)
11	R.O. Ritchie S. Suresh	*Mechanics and physics of the growth of small cracks.* *Behaviour of short cracks in airframe components.* AGARD conference proceedings AGARD-CP-328 (1982)

REFERENCES (continued)

No.	Author	Title, etc
12	K. Tanaka	Mechanisms and mechanics of short fatigue crack propagation. *JSME Int. J.* **30**, No. 259 pp 1-13 (1987)
13	C.J. Mazur J.L. Rudd	*Determination of the short crack effect in 2090-T8E41 aluminium lithium.* *Short-crack growth behaviour in various aircraft materials.* AGARD Report AGARD-R-767 (1990)
14	W.T. Chang K.J. Miller	Elastic-plastic finite element analyses of short cracks. *Fat. Eng. Mat. & Str.* **5**, No. 3 pp 249-263 (1982)
15	R.O. Ritchie W. Yu D.K. Holm A.F. Blom	*Development of fatigue crack closure with the extension of long and short cracks in aluminium alloy 2124: A comparison of experimental and numerical results.* *Mechanics of fatigue crack closure.* ASTM STP 982 (1988)
16	J. Zhang	*A comparison of short and long cracks under monotonic loading using an elastic-plastic finite element method.*
17	P.R. Edwards	*Control and monitoring of servo-hydraulic fatigue machines using a computer network with adaptive control of amplitude and frequency.* Measurement and fatigue-EIS '86 pp 3-17 Pub. EMAS (1986)
18	Various authors	*Description of a fighter aircraft loading standard for fatigue evaluation 'FALSTAFF'.* Common report of F+W Emmen, LBF, NLR, IABG (1976)
19	M. Hück W. Schütz R. Fischer H.G. Kobler	*A standard random load sequence of Gaussian type recommended for general application in fatigue testing.* LBF Report No. 2909. IABG Report No. TF 570 (1976)
20	P.R. Edwards J. Darts	*Standardised fatigue loading sequences for helicopter rotors (Helix and Felix).* RAE Technical Report 84084 Parts 1 and 2 (1984)
21	M.H. Swain J.C. Newman Jr.	*On the use of marker loads and replicas for measuring growth rates for small cracks.* *Behaviour of short cracks in airframe components.* AGARD conference proceedings AGARD-CP-328 (1982)

REFERENCES (concluded)

No.	Author	Title, etc
22	J.C. Newman Jr.	*A crack-closure model for predicting fatigue crack growth under aircraft spectrum loading.* *Methods and models for predicting fatigue crack growth under random loading.* ASTM STP 748 (1981)
23	C.M. Hudson	*Effect of stress ratio on fatigue-crack growth in 7075-T6 and 2024-T3 aluminium alloy specimens.* NASA TND-5390 (1969)
24	E.P. Phillips	*The influence of crack closure on fatigue crack growth thresholds in 2024-T3 aluminium alloy. Mechanics of fatigue crack closure.* ASTM STP 982 (1988)
25	J.C. Newman Jr.	A crack opening stress equation for fatigue crack growth. *Int. J. of Fracture* **24,** R131-R135 (1984)

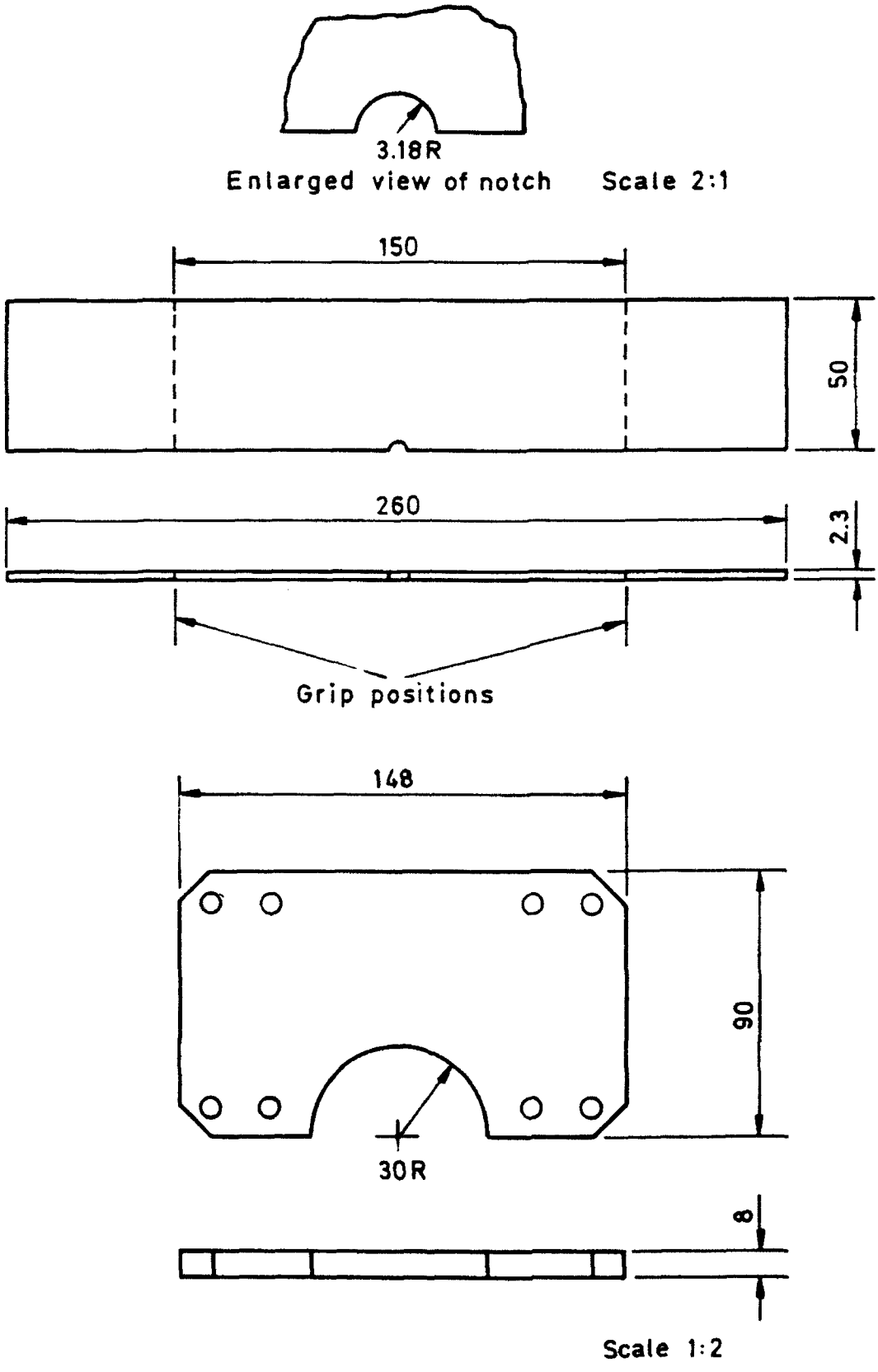

Fig 1 Short crack specimen and anti-buckling guide

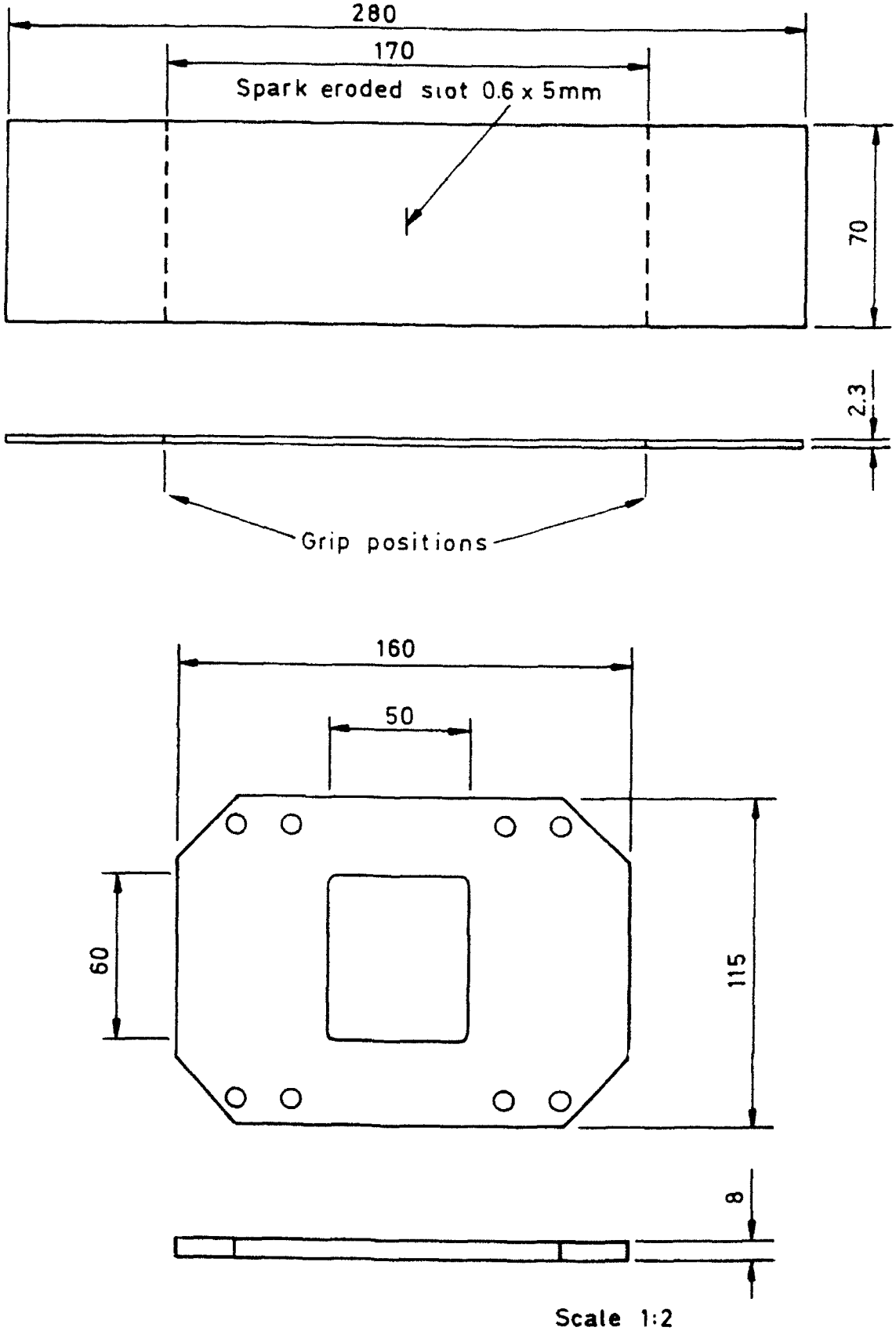

Fig 2 Long crack specimen and anti-buckling guide

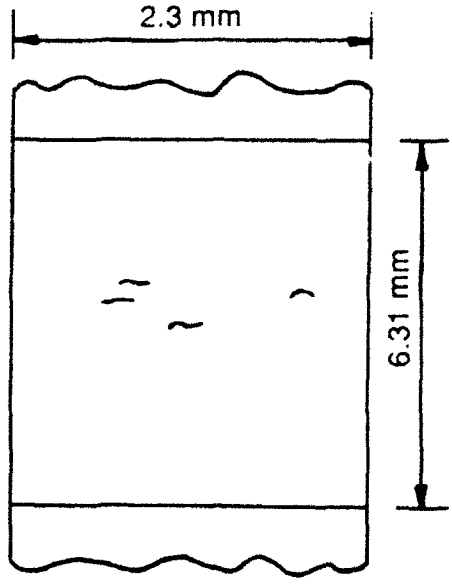

a) Multiple cracks in side notch specimen

AGARD Short crack activity
Record of crack lengths and map

Page 3 of 6 Loading action C/A R = -2
Specimen No A-72-09 Peak stress 50 MPa

0.1 mm grid

157500 Cycles
L1 0.22 mm
L2 L1 mm
L3 0.18 mm
L4 0.17 mm
L5 0.24 mm

165000 Cycles
L1 0.24 mm
L2 L1 mm
L3 0.18 mm
L4 0.17 mm
L5 0.27 mm

172500 Cycles
L1 0.25 mm
L2 L1 mm
L3 0.31 mm
L4 0.17 mm
L5 0.30 mm

180000 Cycles
L1 0.28 mm
L2 L1 mm
L3 0.55 mm
L4 0.17 mm
L5 0.33 mm

187500 Cycles
L1 0.32 mm
L2 L1 mm
L3 0.55 mm
L4 L3 mm
L5 0.38 mm

195000 Cycles
L1 0.34 mm
L2 L1 mm
L3 0.58 mm
L4 L3 mm
L5 0.43 mm

b) Data chart for above test

Fig 3 Short crack measurement records

Fig 4

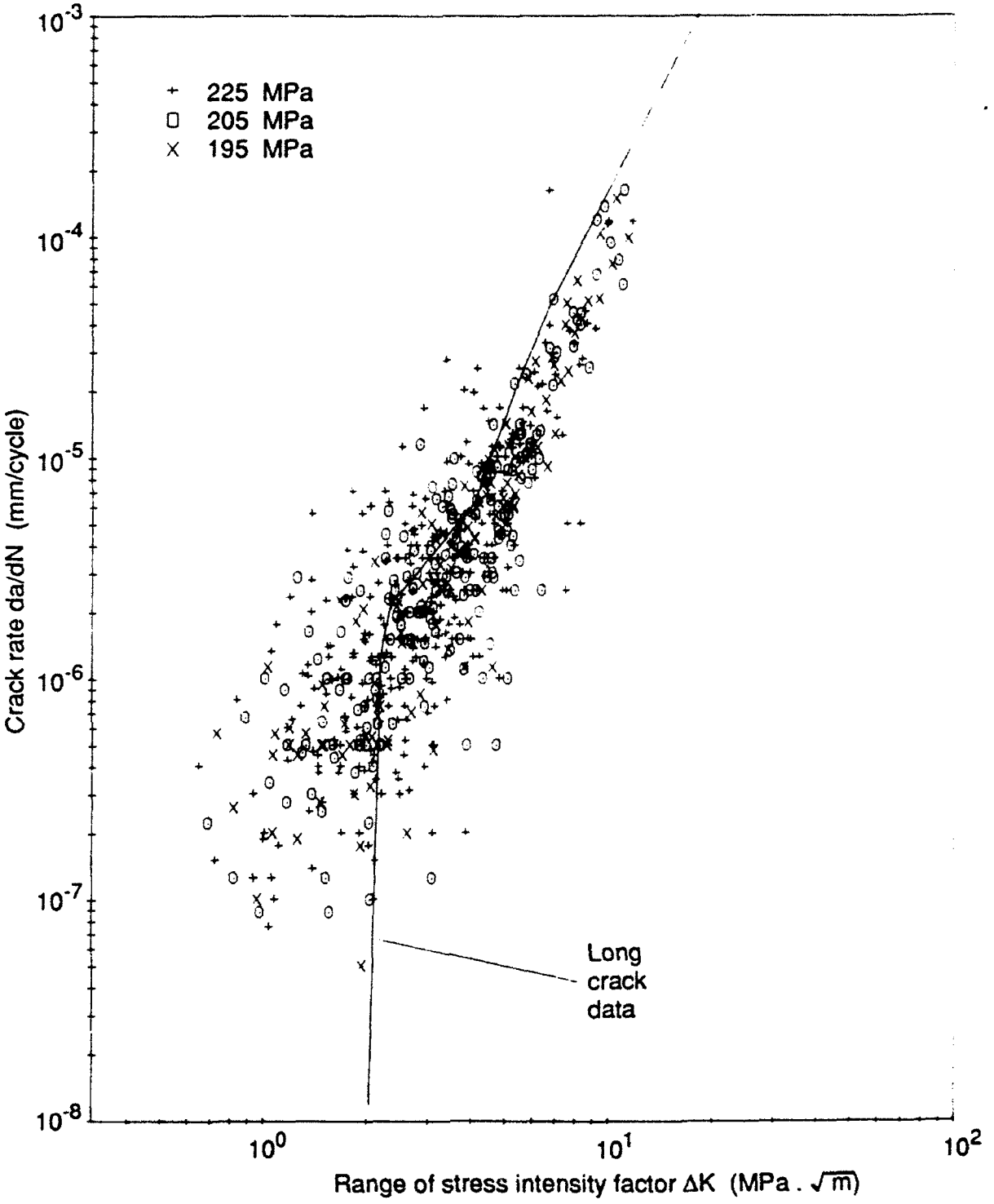

Fig 4 Short and long crack growth data under constant amplitude R = 0.5 loading

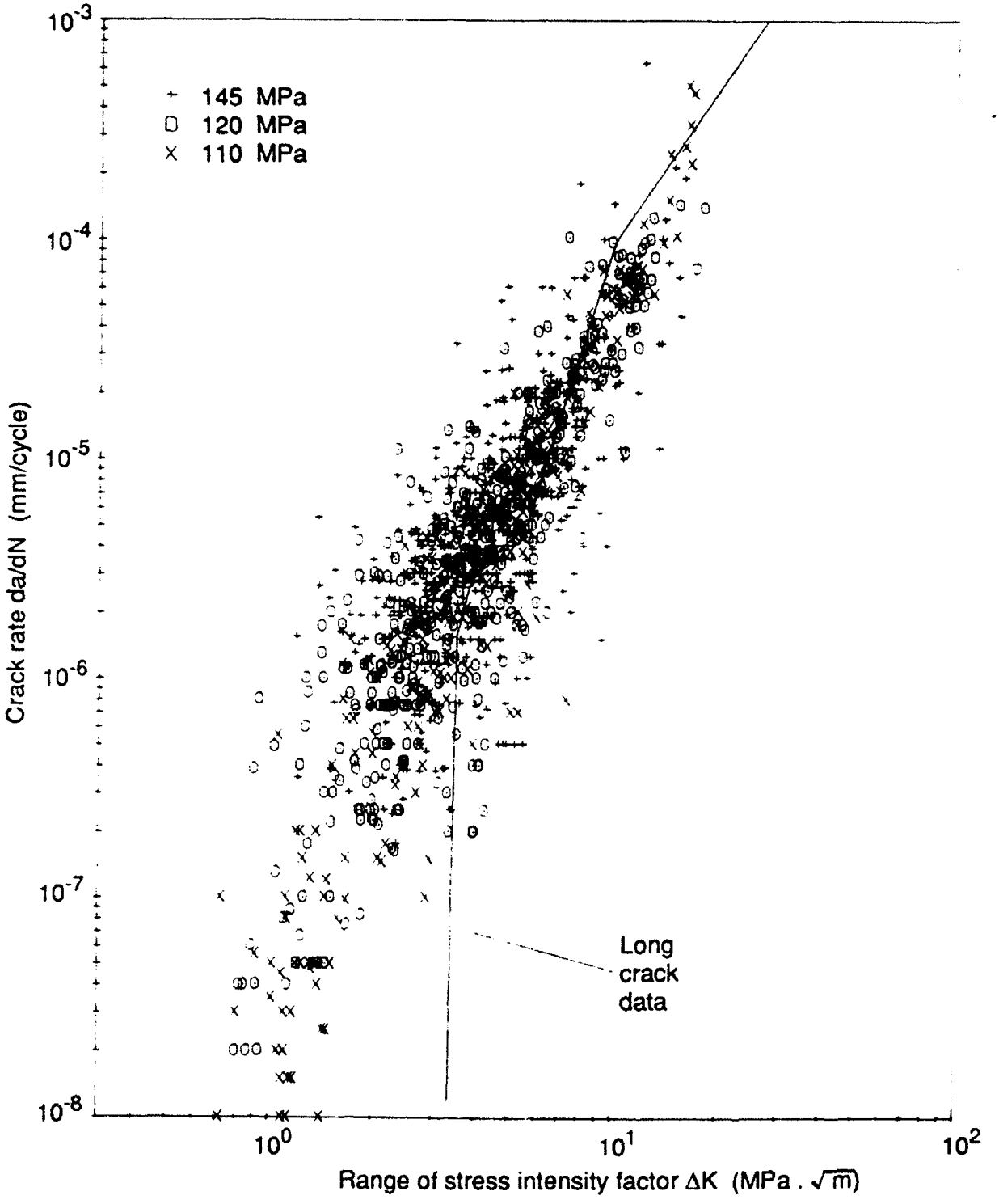

Fig 5 Short and long crack growth data under constant amplitude R = 0 loading

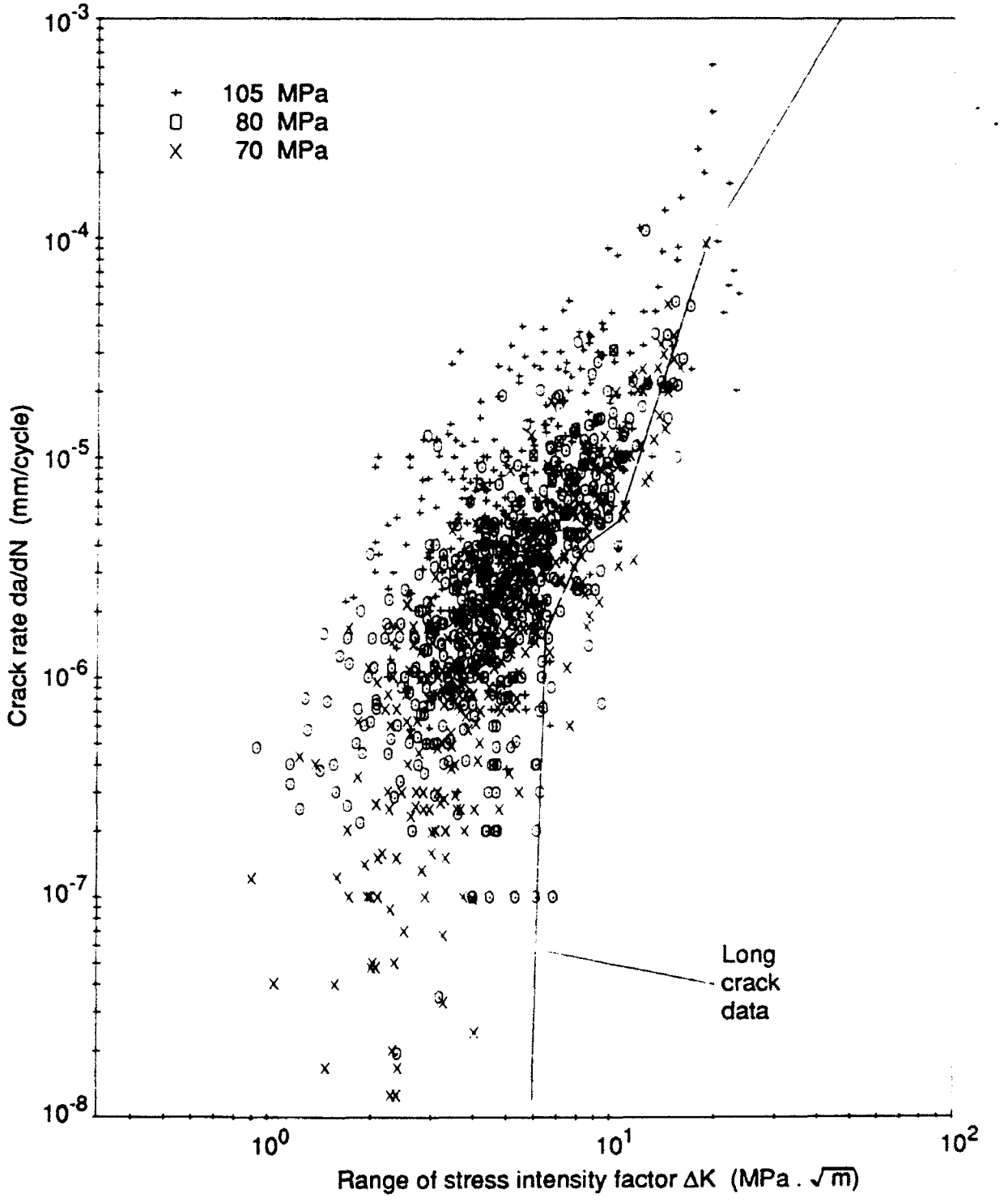

Fig 6 Short and long crack growth data under constant amplitude R = -1 loading

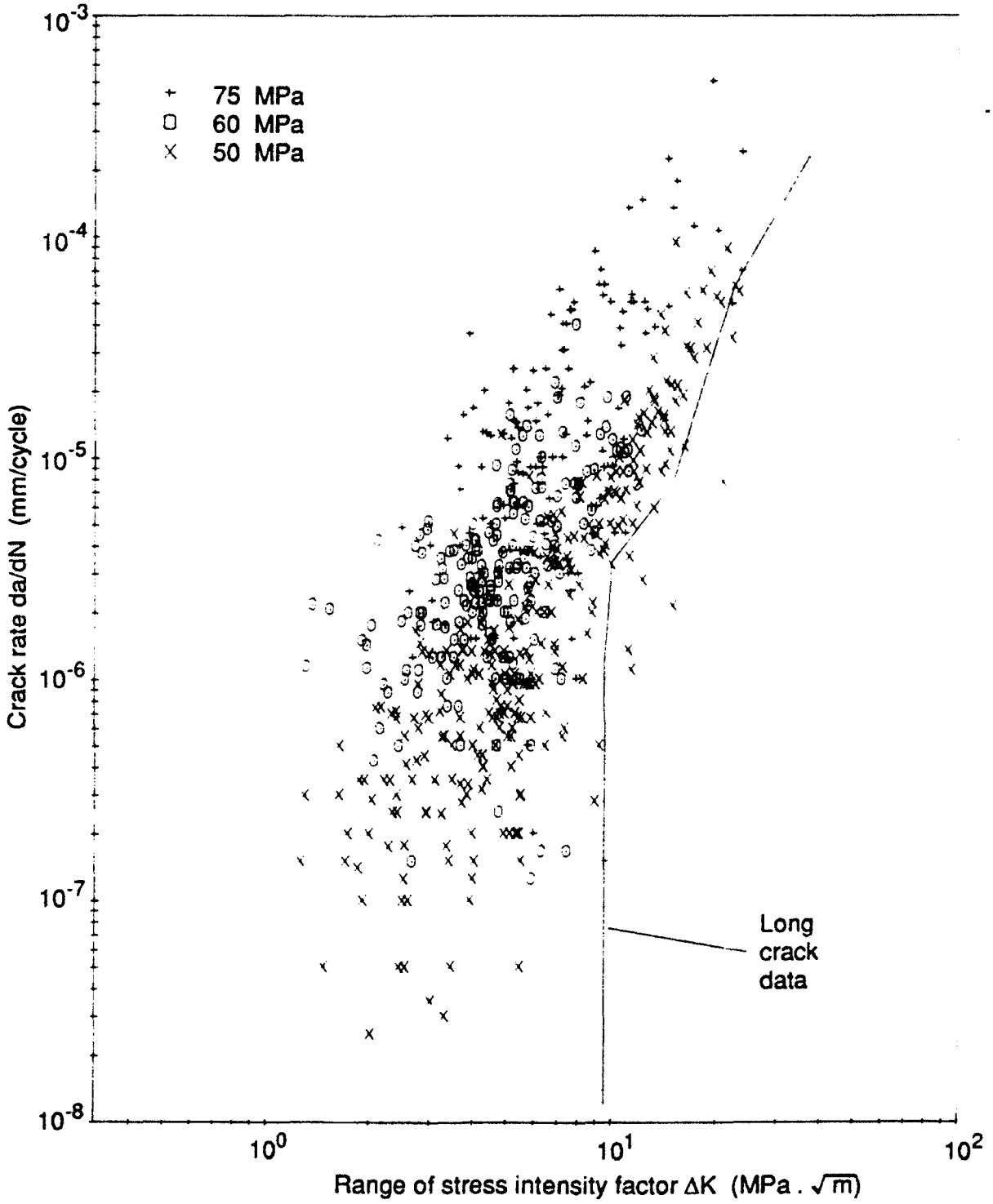

Fig 7 Short and long crack growth data under constant amplitude R = -2 loading

Fig 8

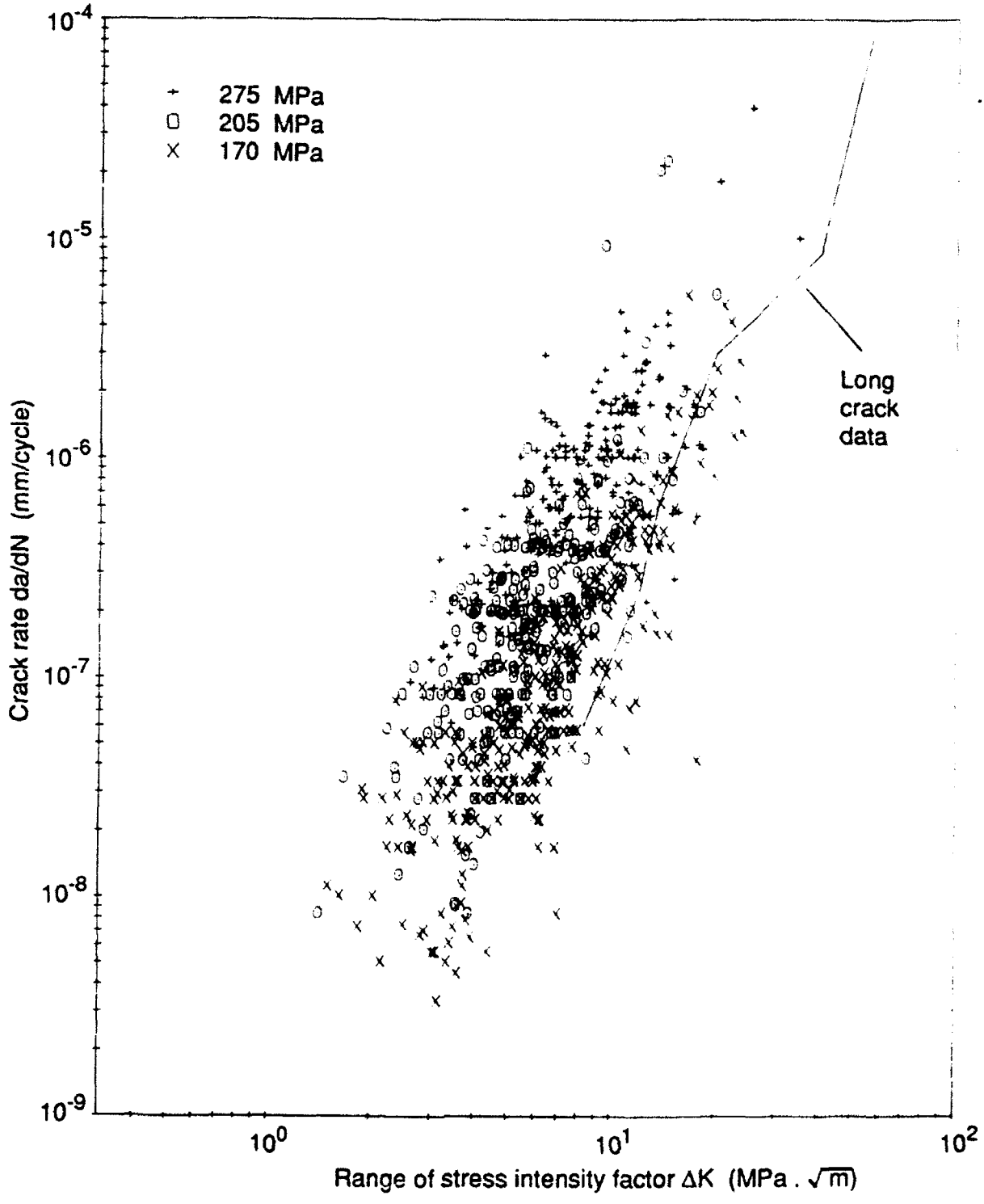

Fig 8 Short and long crack growth data under FALSTAFF loading

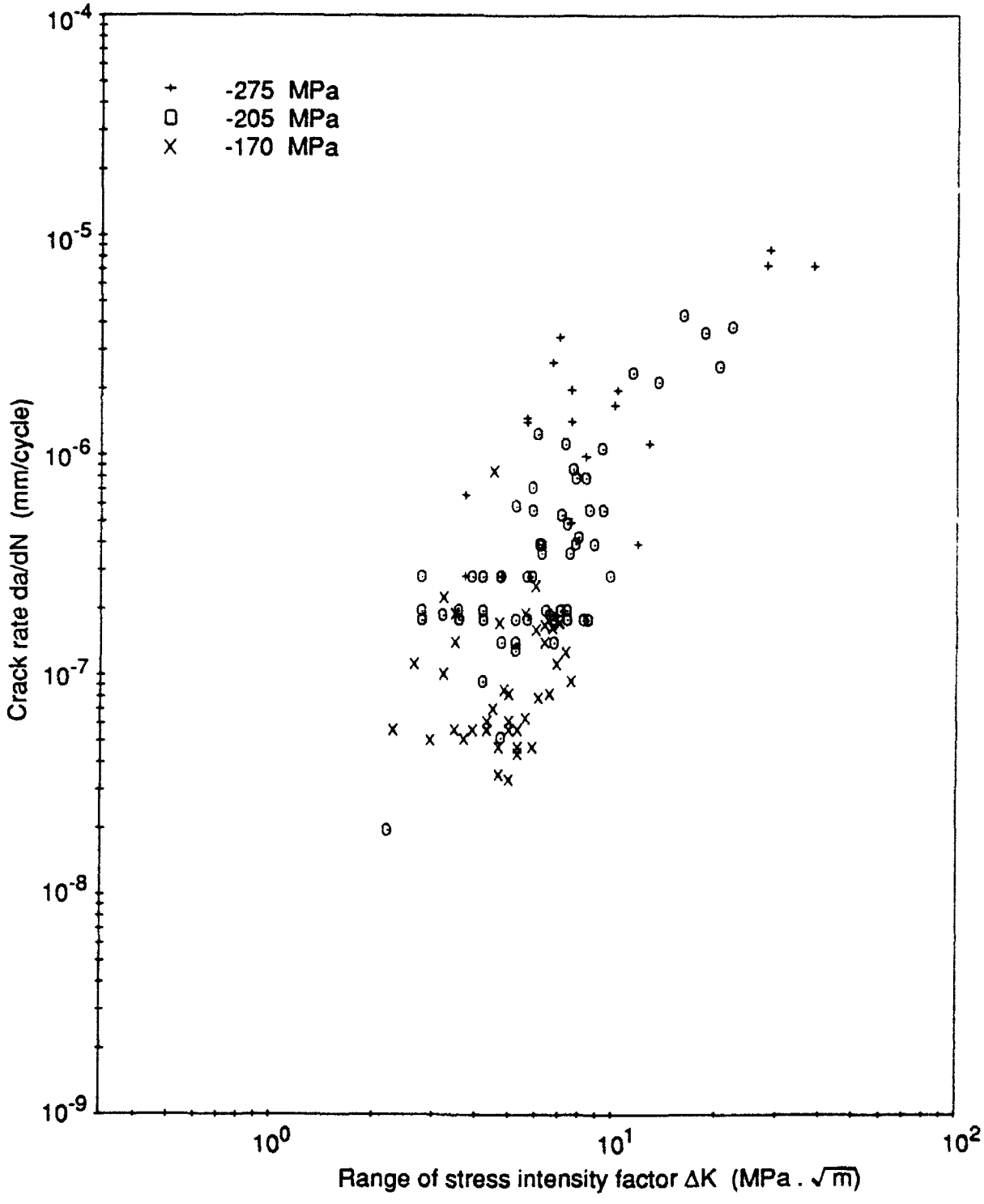

Fig 9 Short crack growth data under inverted FALSTAFF loading

Fig 10

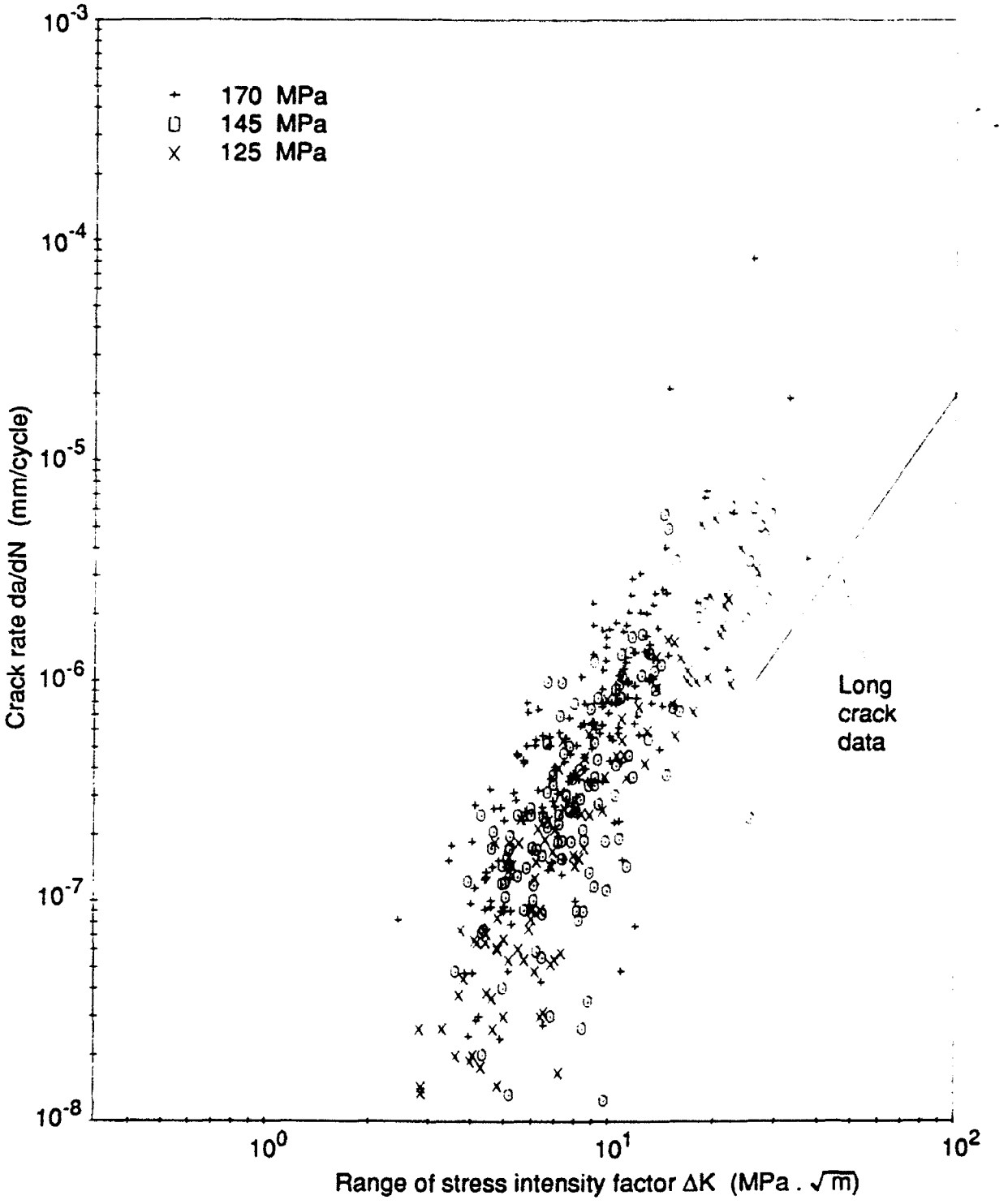

Fig 10 Short and long crack growth data under Gaussian loading

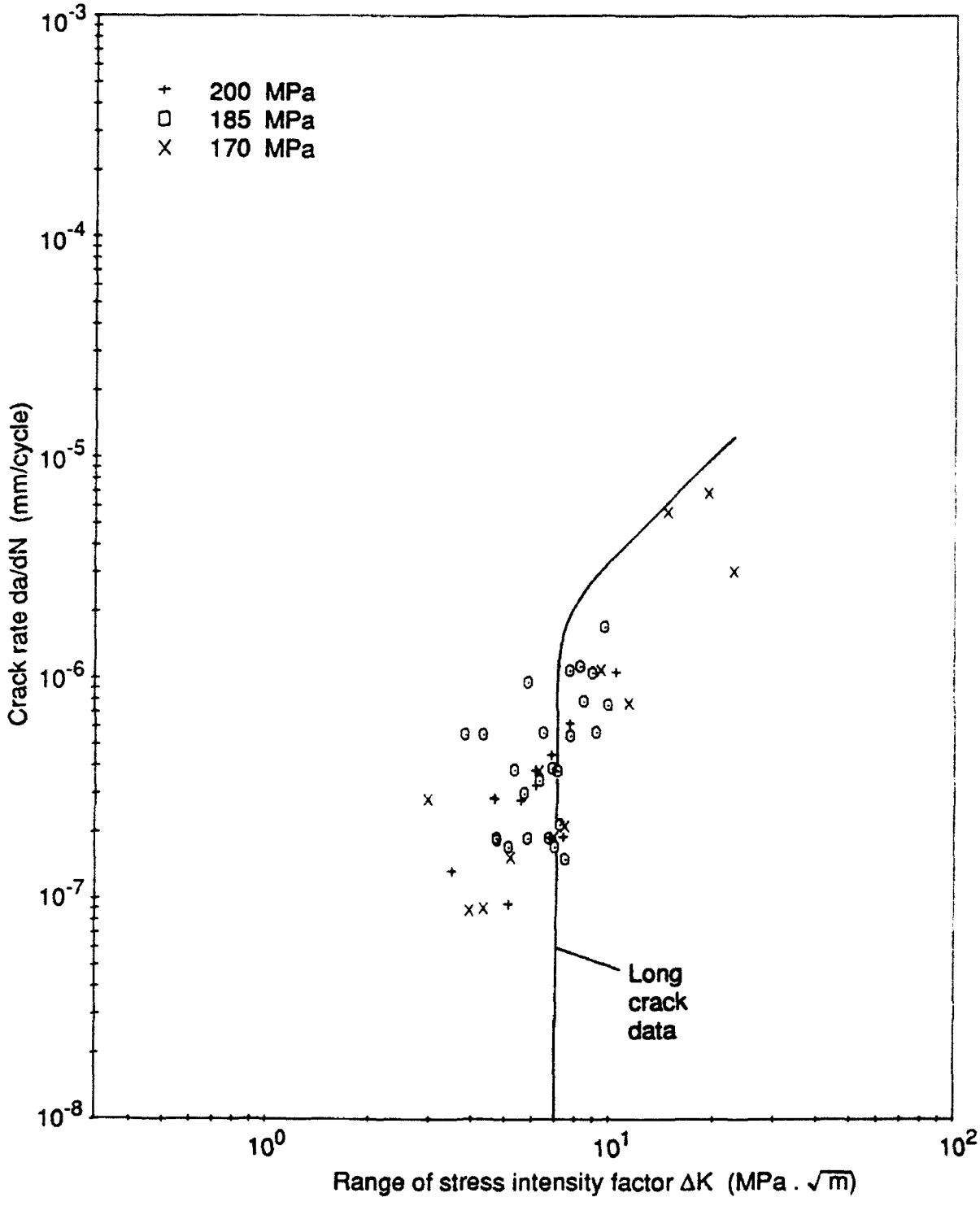

Fig 11 Short and long crack growth data under Felix loading

Fig 12

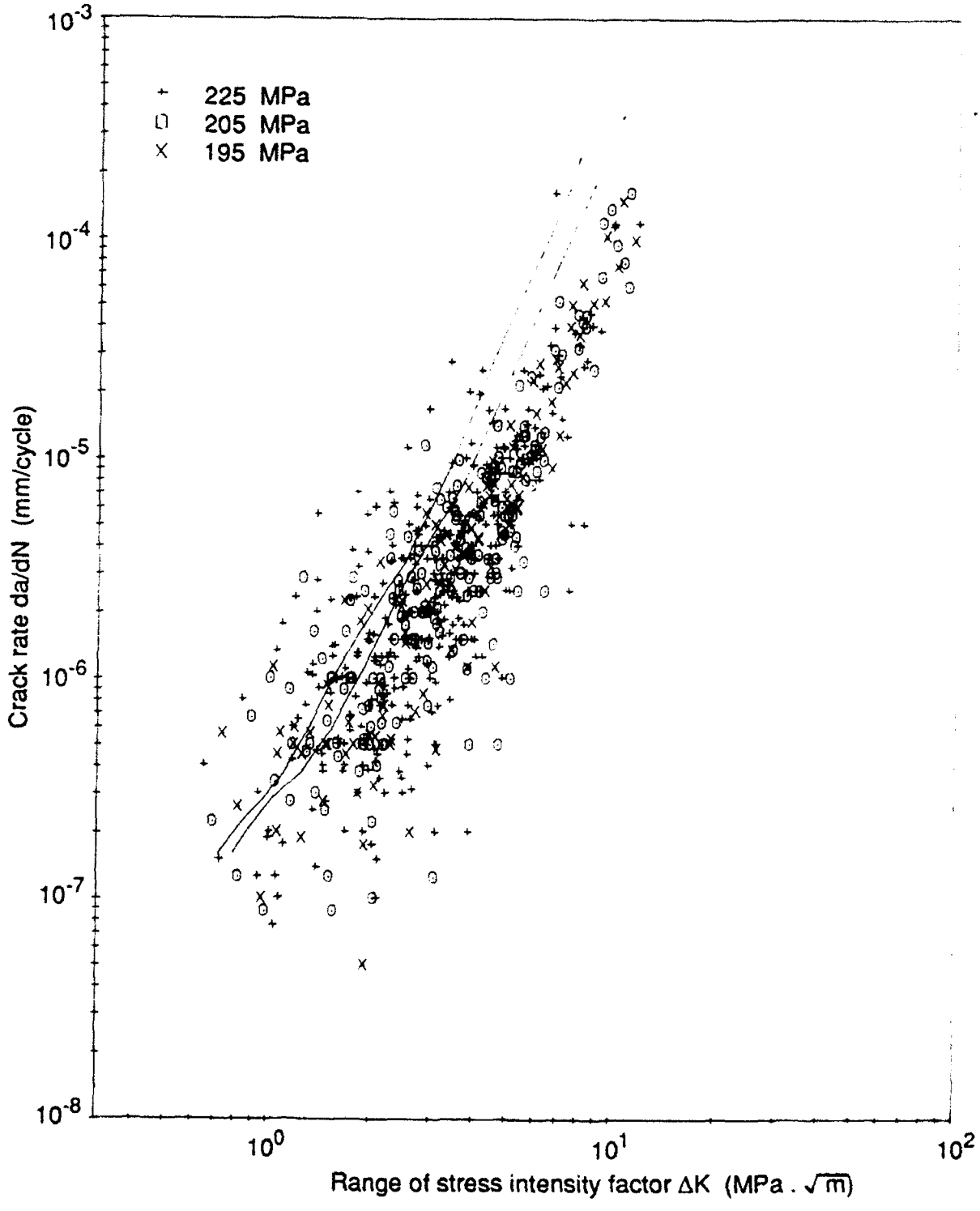

Fig 12 Predicted and measured crack growth rates under constant amplitude R = 0.5 loading

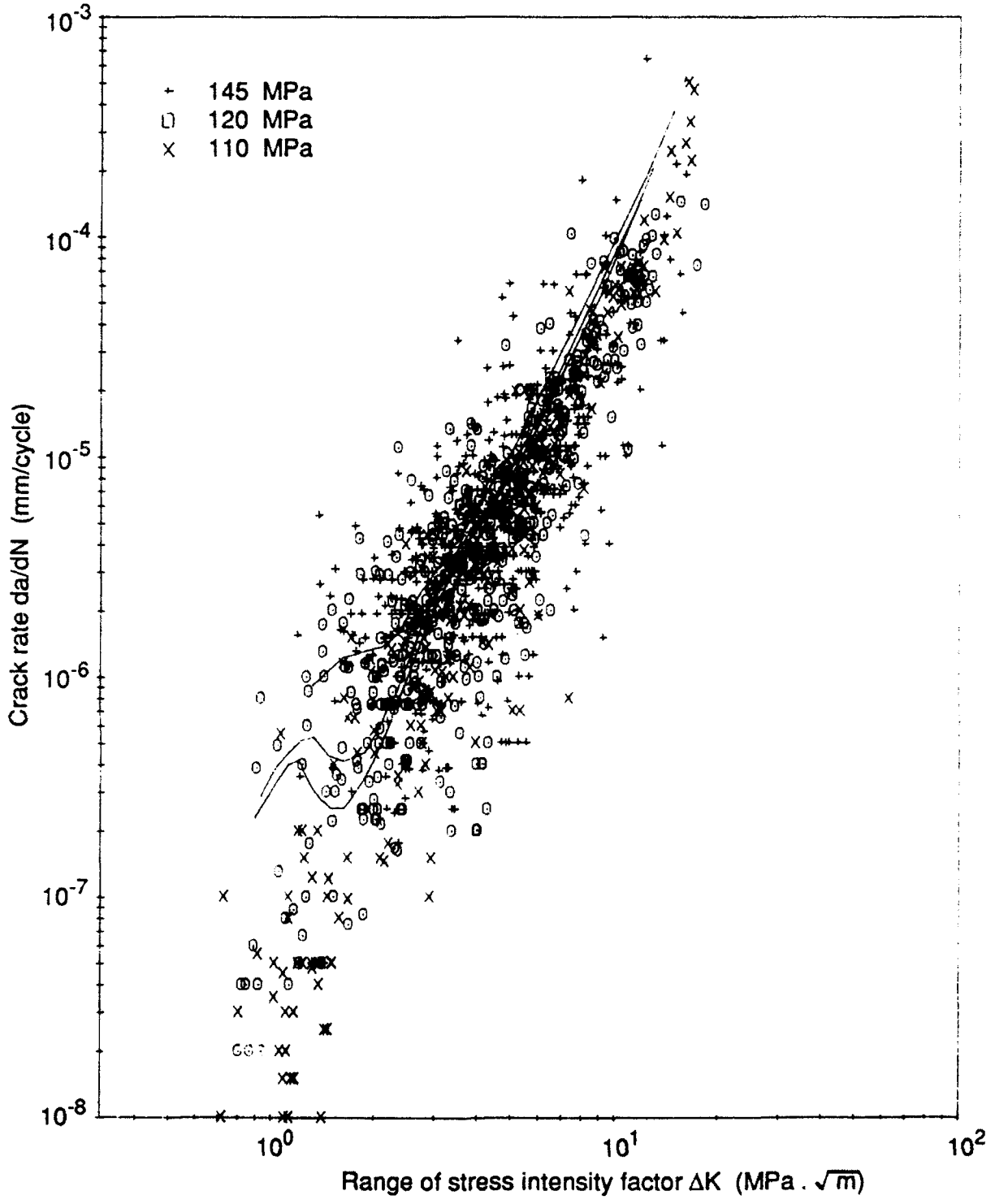

Fig 13 Predicted and measured crack growth rates under constant amplitude R = 0 loading

Fig 14

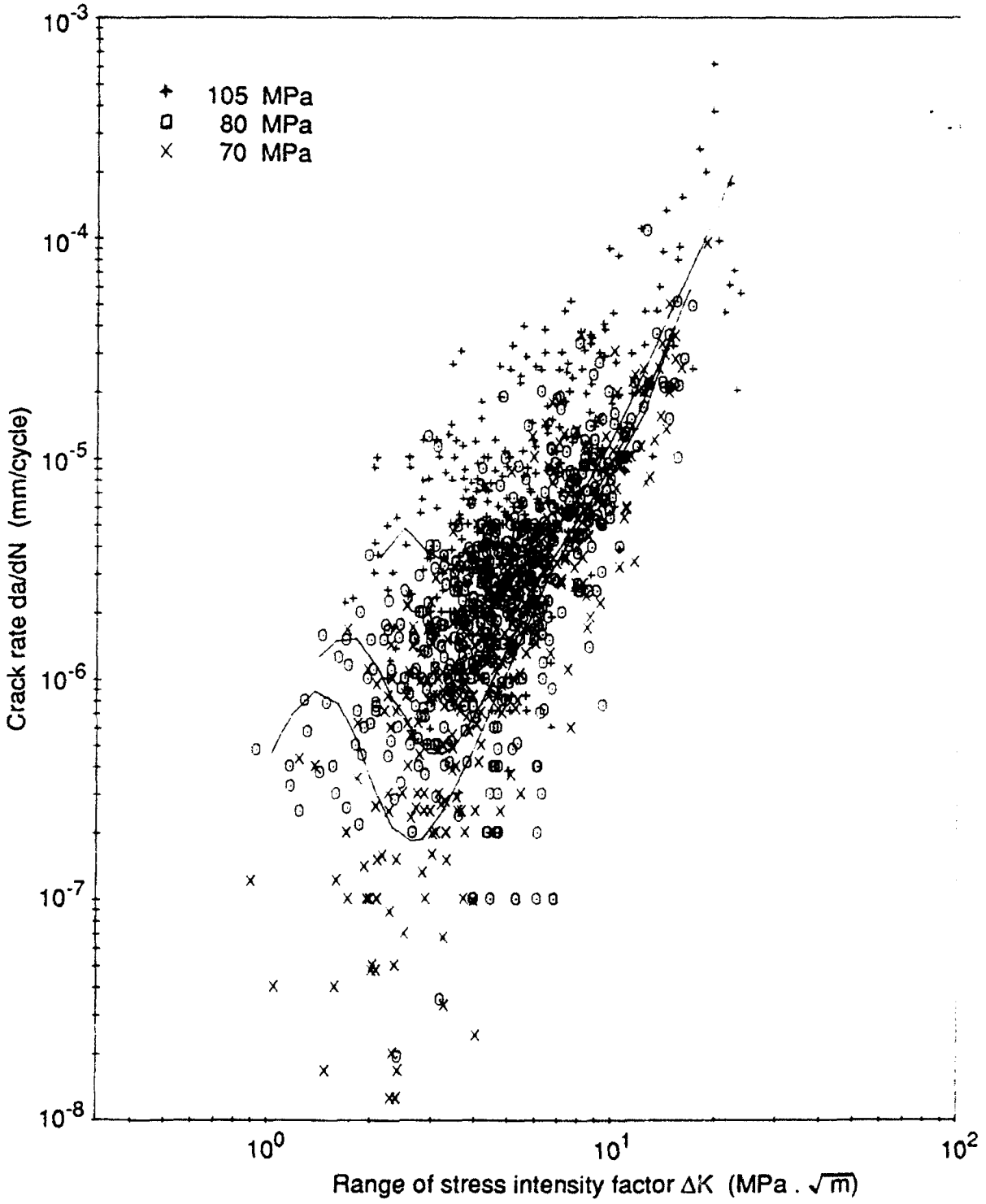

Fig 14 Predicted and measured crack growth rates under constant amplitude R = -1 loading

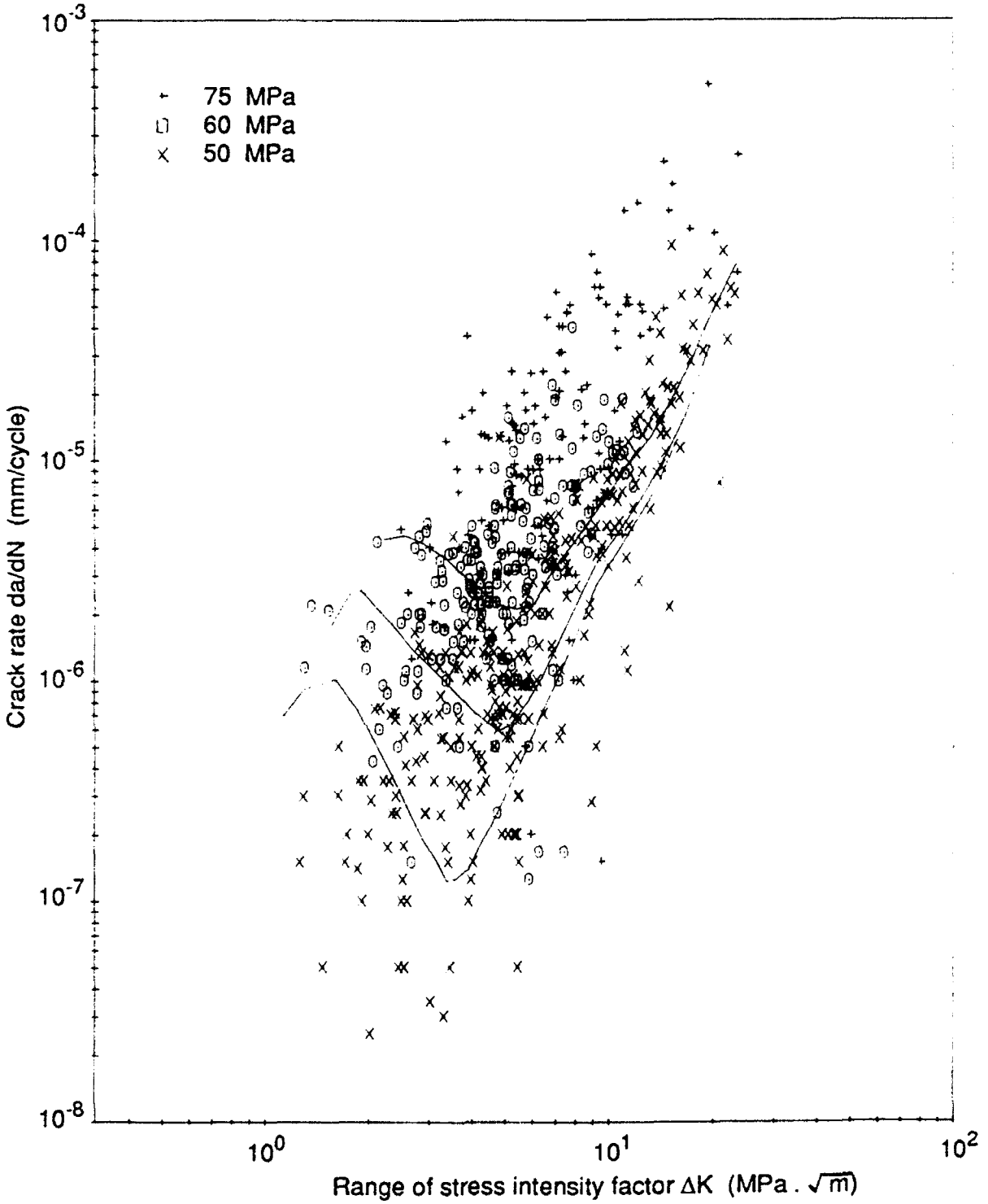

Fig 15 Predicted and measured crack growth rates under constant amplitude R = -2 loading

Fig 16

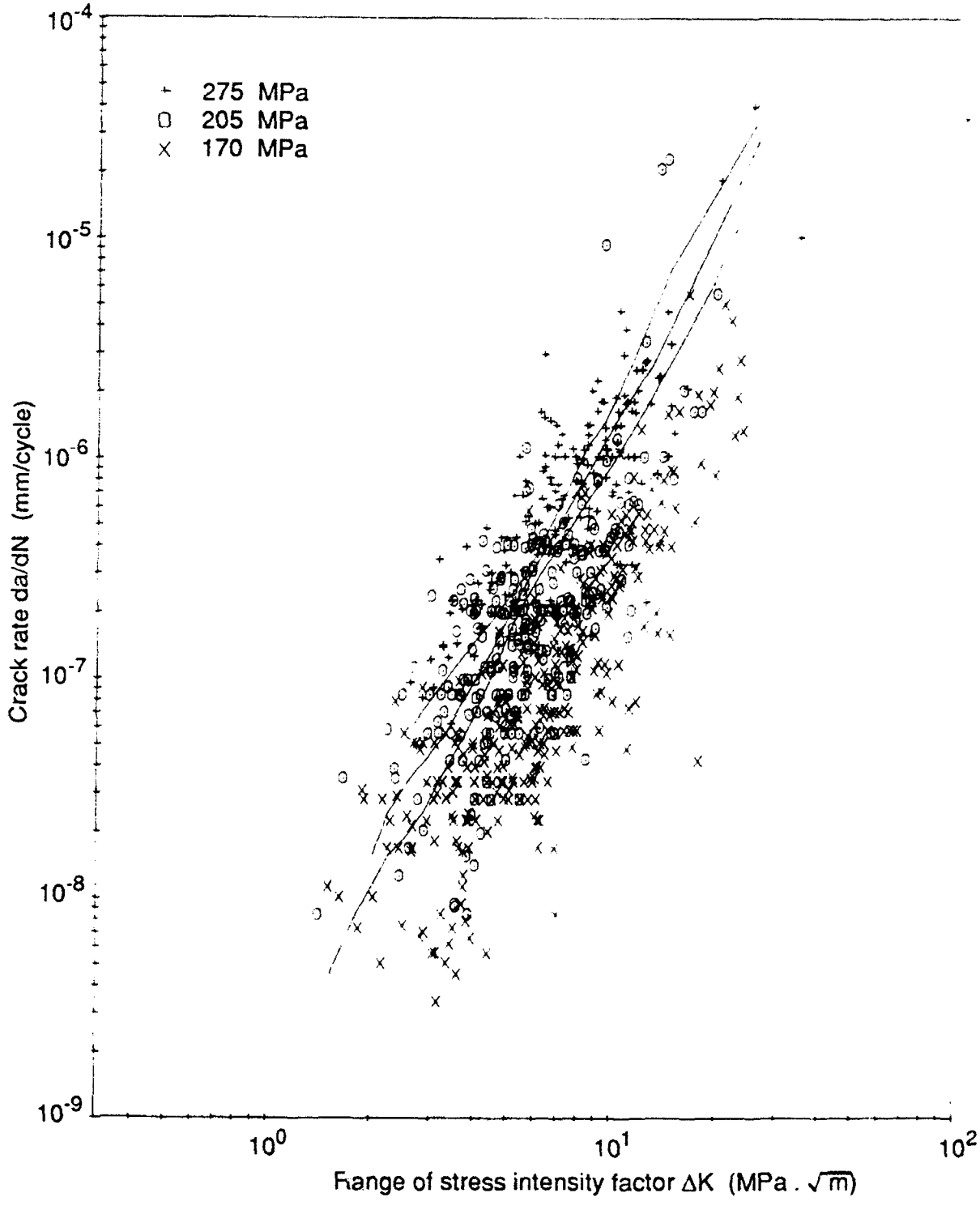

Fig 16 Predicted and measured crack growth rates under FALSTAFF loading

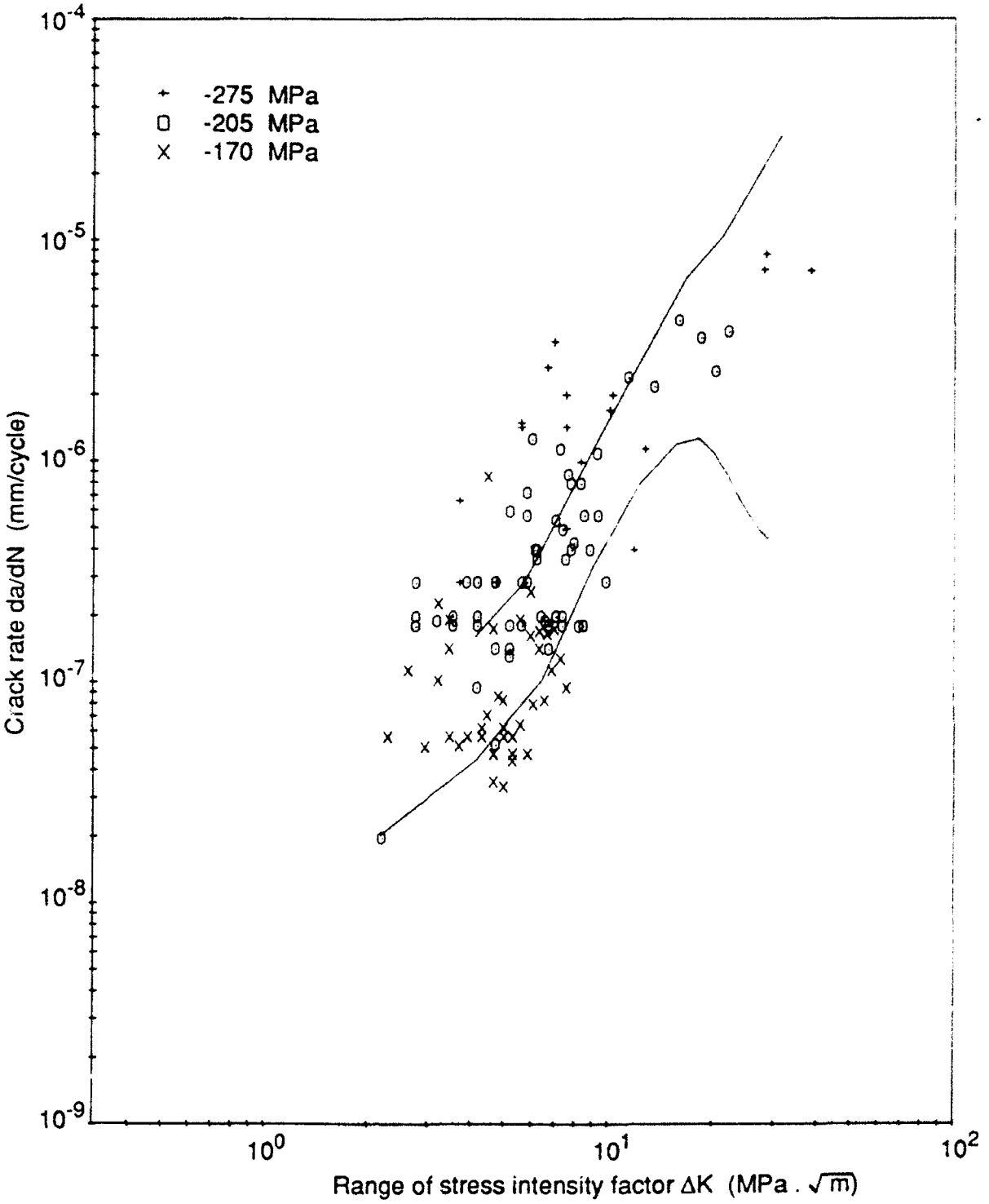

Fig 17 Predicted and measured crack growth rates under inverted FALSTAFF loading

Fig 18

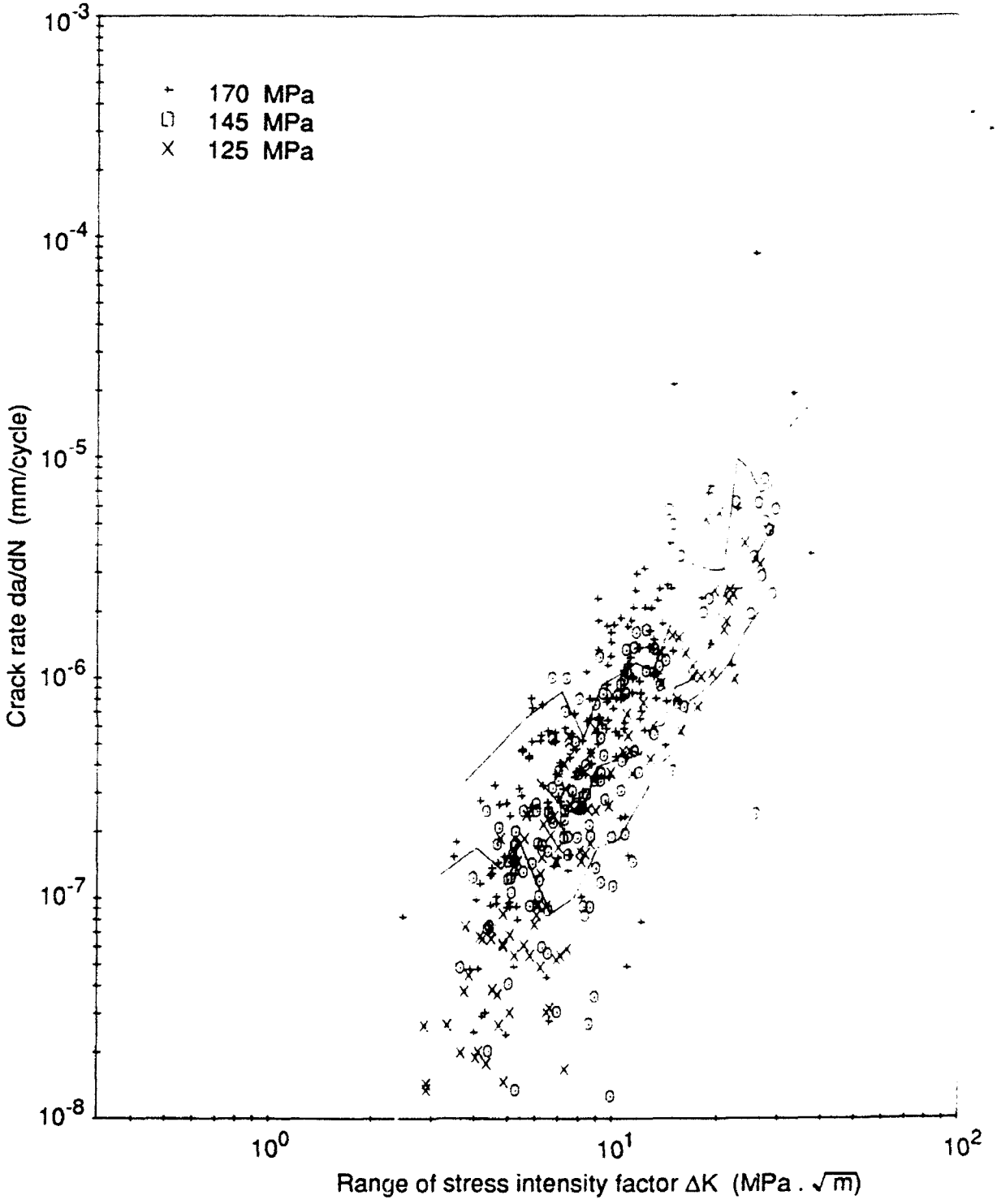

Fig 18 Predicted and measured crack growth rates under Gaussian loading

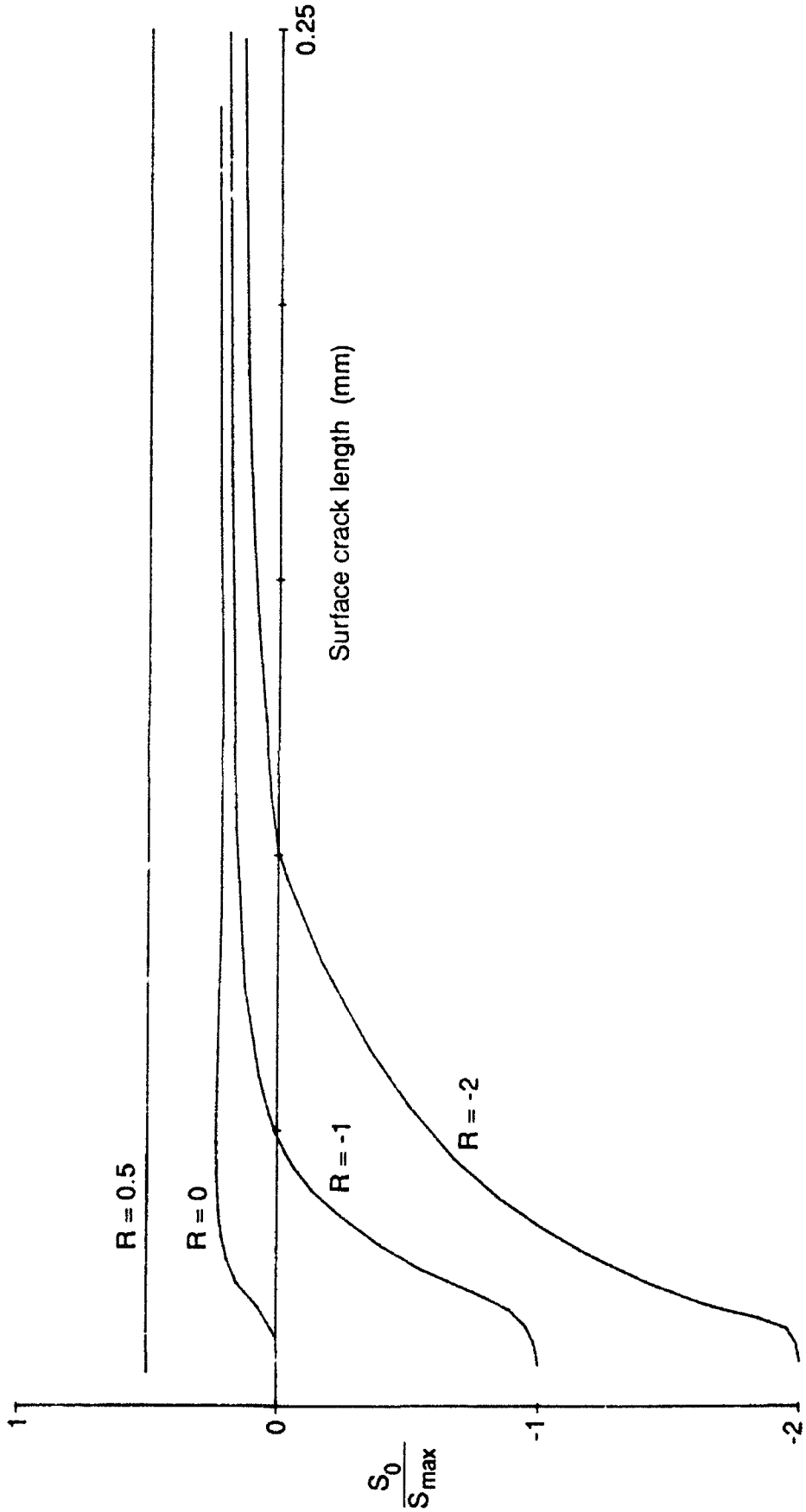

Fig 19 Predicted crack closure levels for constant amplitude loading

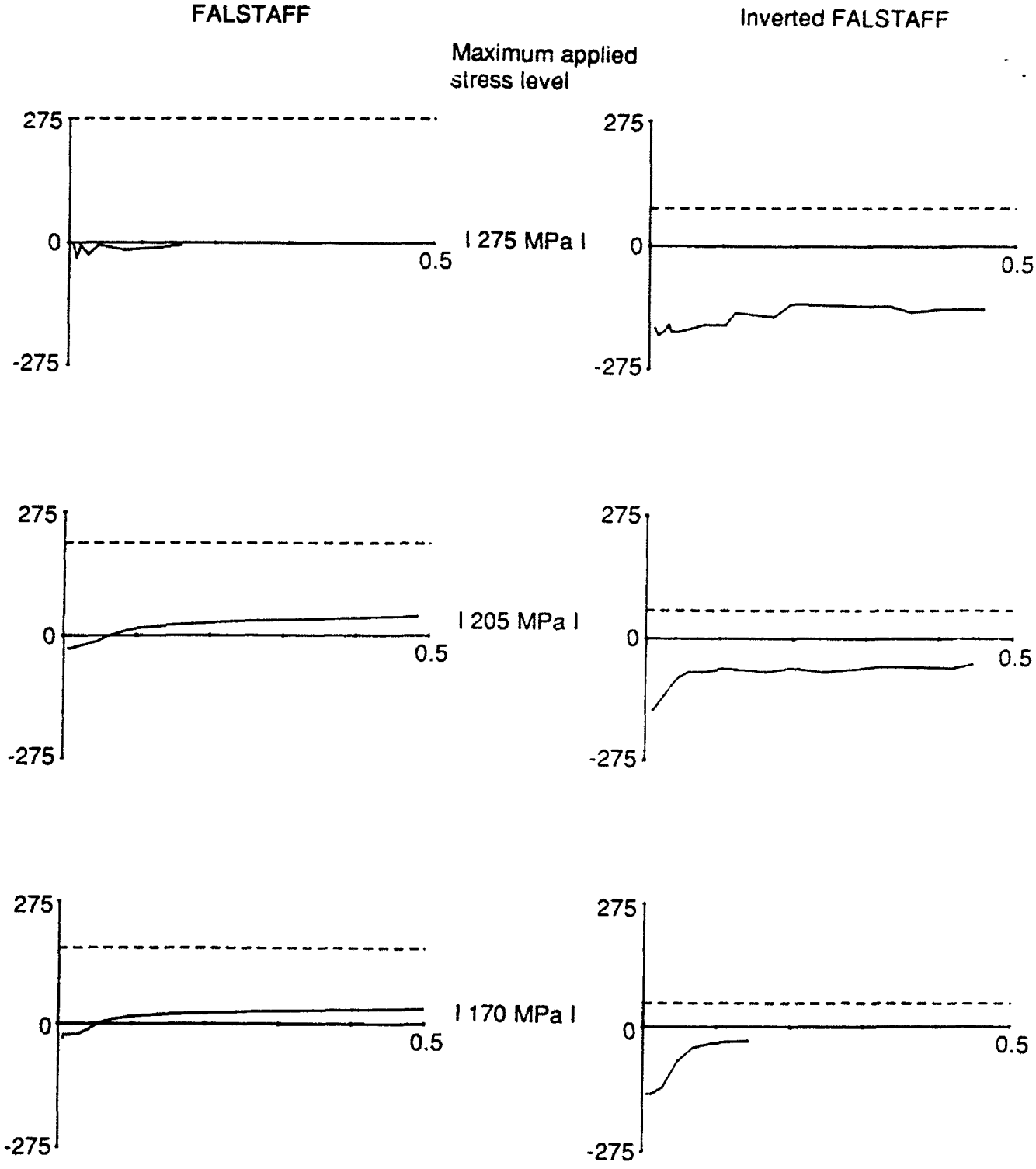

Fig 20 Predicted crack closure levels for FALSTAFF and Inverted FALSTAFF loading

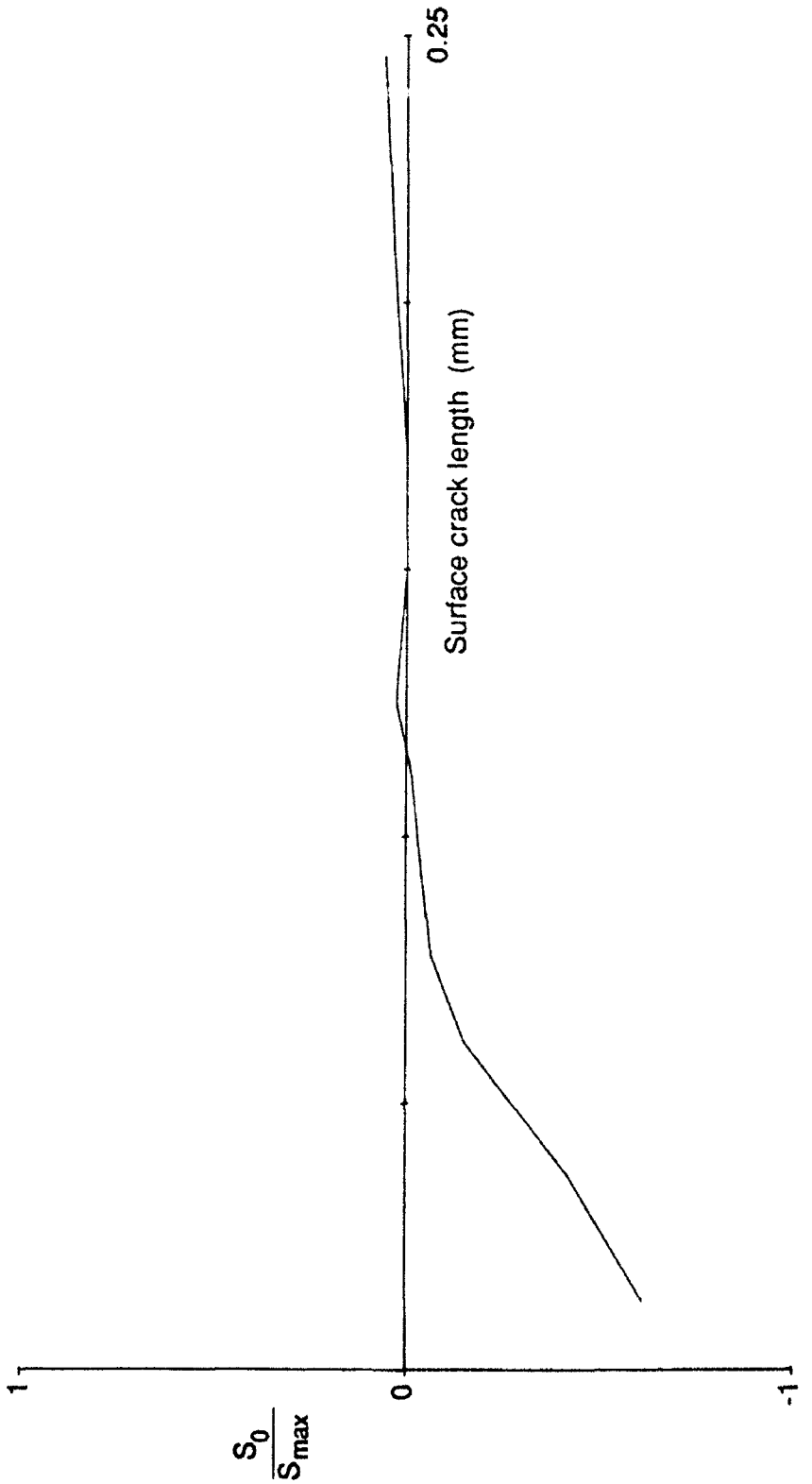

Fig 21 Predicted crack closure levels for Gaussian loading

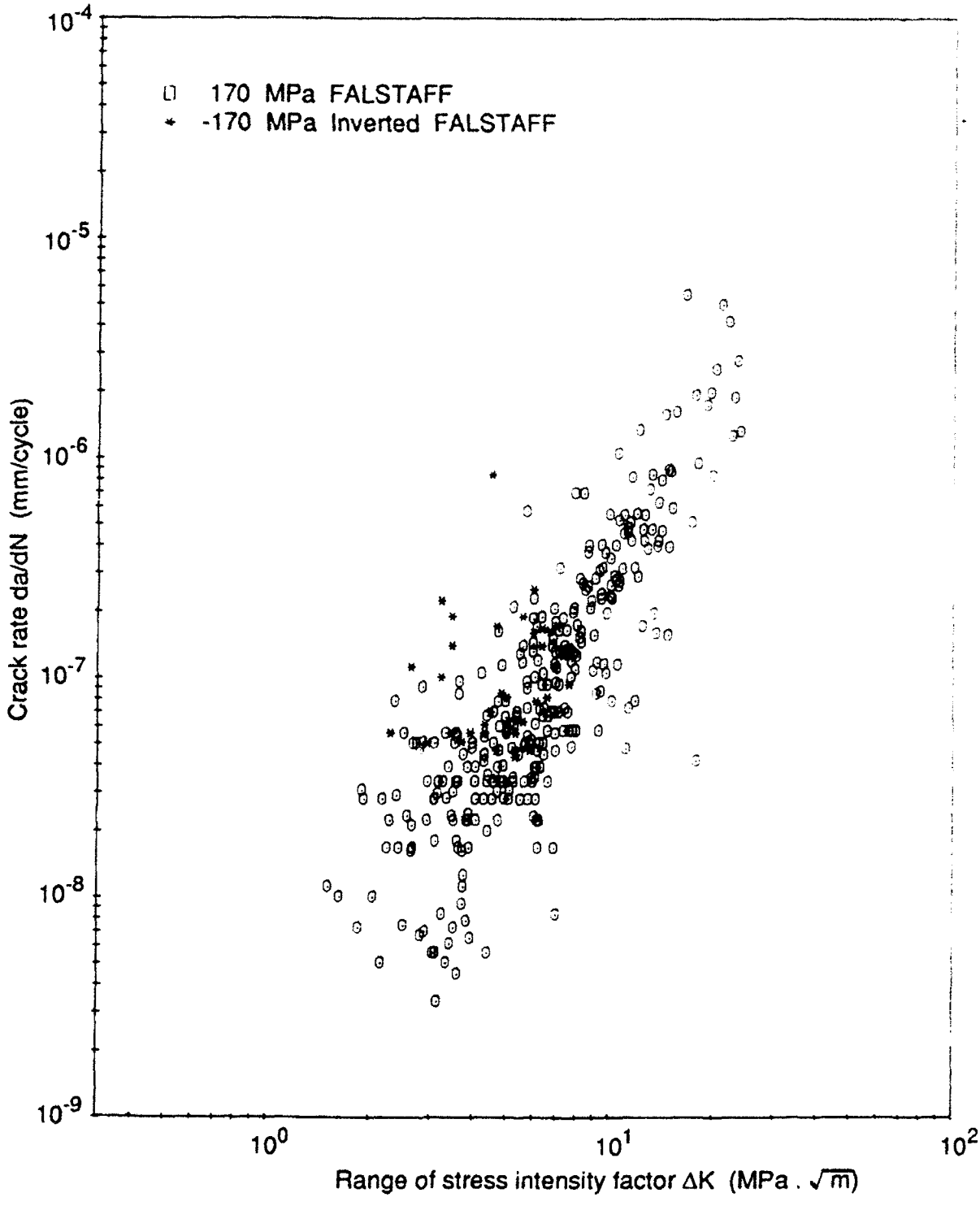

Fig 22 Short crack growth rates under FALSTAFF and Inverted FALSTAFF loading at a peak stress level of I170 MPa I

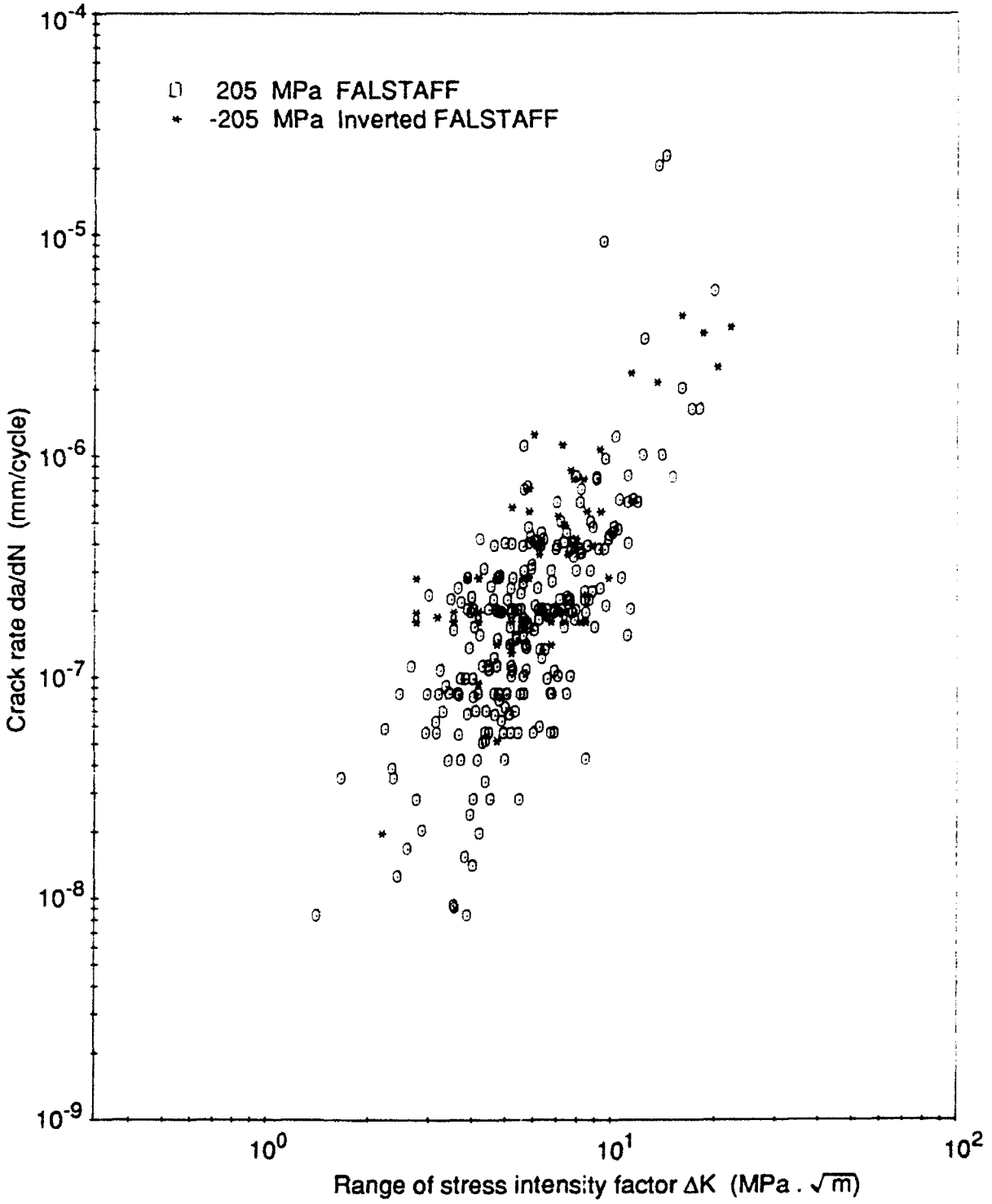

Fig 23 Short crack growth rates under FALSTAFF and Inverted FALSTAFF loading at a peak stress level of ǀ 205 MPa ǀ

Fig 24

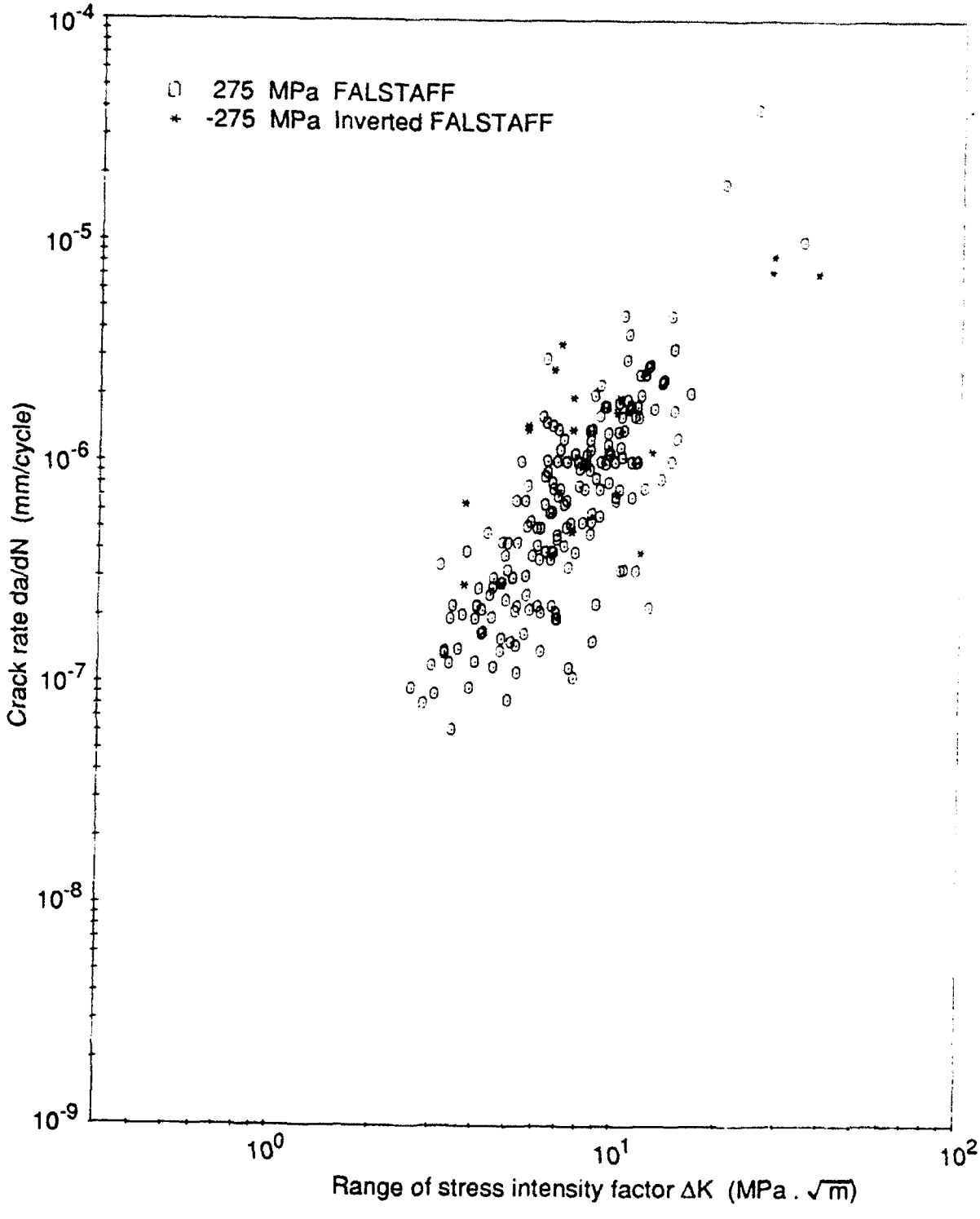

Fig 24 Short crack growth rates under FALSTAFF and Inverted FALSTAFF loading at a peak stress level of ! 275 MPa !

DEFENCE RESEARCH AGENCY

REPORT DOCUMENTATION PAGE

Overall security classification of this page

UNLIMITED

As far as possible this page should contain only unclassified information. If it is necessary to enter classified information, the box above must be marked to indicate the classification, *eg* Restricted, Confidential or Secret.

1. DRIC Reference (to be added by DRIC)	2. Originator's Reference	3. Agency Reference	4. Report Security Classification/Marking
	DRA TR 92063	N/A	UNLIMITED

5. DRIC Code for Originator	6. Originator (Corporate Author) Name and Location
7673000W	DRA Farnborough, Hampshire, GU14 6TD
5a. Sponsoring Agency's Code	6a. Sponsoring Agency (Contract Authority) Name and Location
N/A	

7. Title

The Growth of Short Fatigue Cracks in an Aluminium Alloy

7a. (For Translations) Title in Foreign Language

7b. (For Conference Papers) Title, Place and Date of Conference

8. Author 1, Surname, Initials	9a. Author 2	9b. Authors 3,4 ...	10. Date	Pages	Refs
Cook, R.			November 1992	47	25

11. Contract Number	12. Period	13. Project	14. Other Reference Nos.
N/A	N/A		Materials/Structures 363

15. Distribution statement

(a) Controlled by – Unlimited distribution

(b) Special limitations (if any) –

If it is intended that a copy of this document shall be released overseas refer to DRA Leaflet No. 3 to Supplement 6 of MOD Manual 4

16. Descriptors (Keywords) (Descriptors marked * are selected from TEST)

Fatigue. Crack. Crack closure. Fracture mechanics.

17. Abstract

Fatigue tests have been carried out to establish the effects of various constant amplitude and standardised variable amplitude loading sequences on the growth of short and long cracks in 2024-T3 aluminium alloy. In most cases, the growth rates of short cracks were greater than those of long cracks for the same nominal stress intensity factor ranges, and short cracks grew at stress intensity factor ranges below the long crack threshold values. This Report describes and discusses the experimental crack growth results and compares them with predictions based on the FASTRAN crack closure model of Newman. The experimental work reported includes that which represented the United Kingdom contribution to the core programme of the AGARD cooperative programme on short crack growth behaviour.